The CT18 QCD analysis with the LHC experimental data

Pavel Nadolsky

Southern Methodist University

CTEQ-TEA (Tung et al.) working group

China Northeastern University: T.-J. Hou

Kennesaw State University: M. Guzzi

Michigan State U.: J. Huston, J. Pumplin, D. Stump, C. Schmidt, J. Winter, C.-P. Yuan

Shanghai Jiao Tong University: J. Gao

Southern Methodist University: T. Hobbs, P.N., B.T.Wang, K. Xie

Xinjiang University: S. Dulat, I. Sitiwaldi

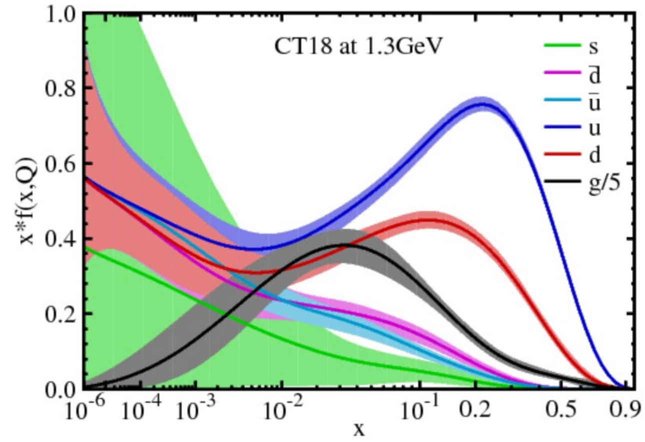

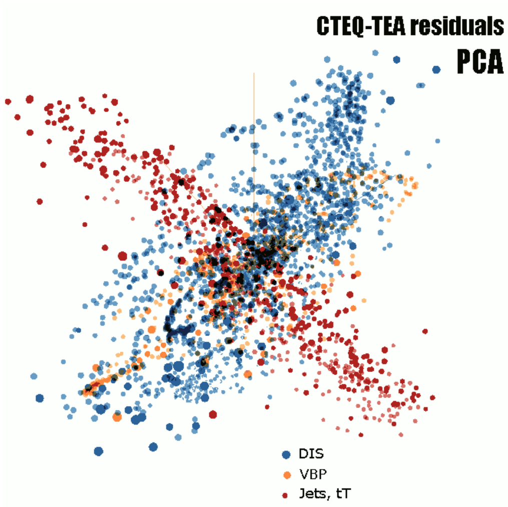

CT18 parton distributions

Four PDF ensembles: CT18 (default), A, X, and Z

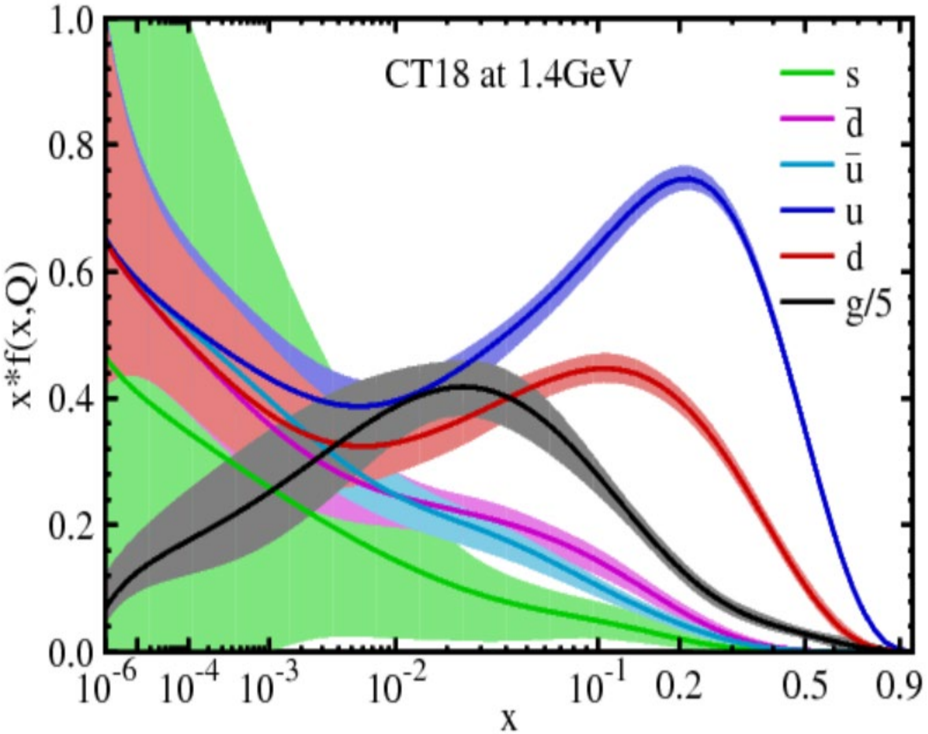

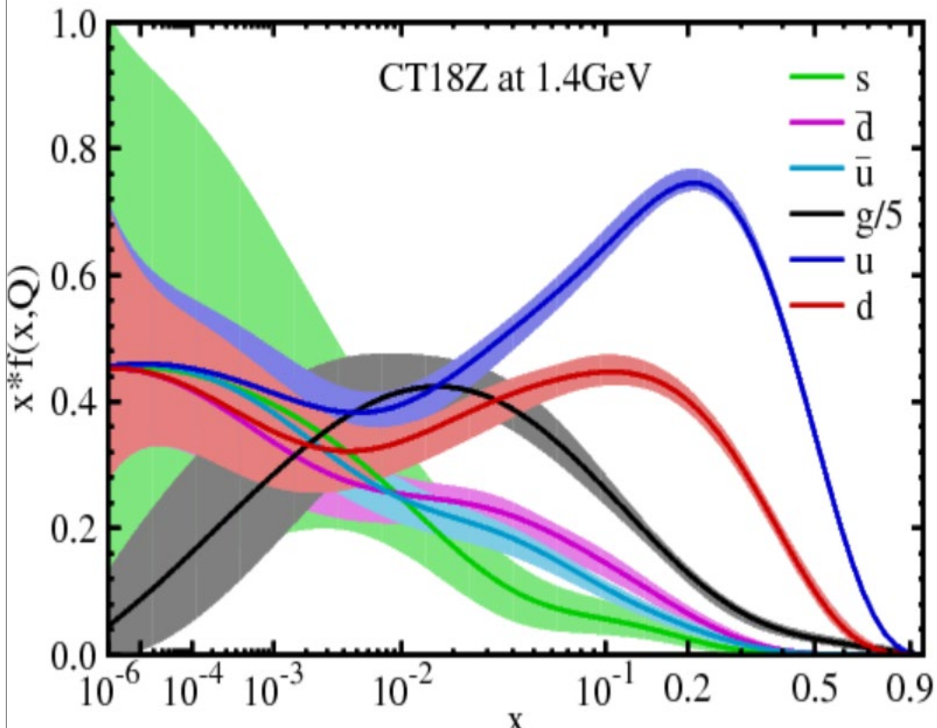

CT18Z has enhanced gluon and strange PDFs at $x \sim 10^{-4}$, and reduced light-quark PDFs at $x < 10^{-2}$. The CT18Z fit is performed so as to maximize the differences from CT18 PDFs, while preserving about the same goodness-of-fit as for CT18. CT18A and CT18X include some features of CT18Z

CT18/CT18Z parton luminosities

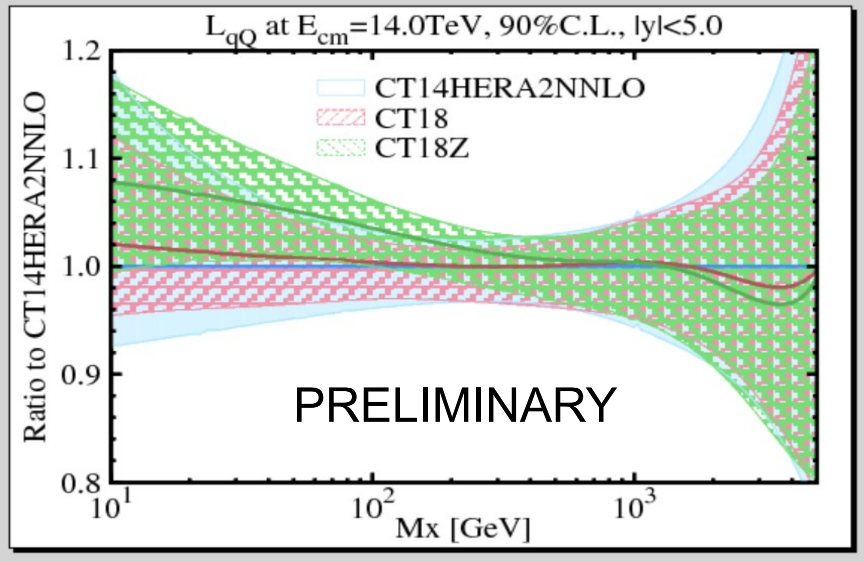

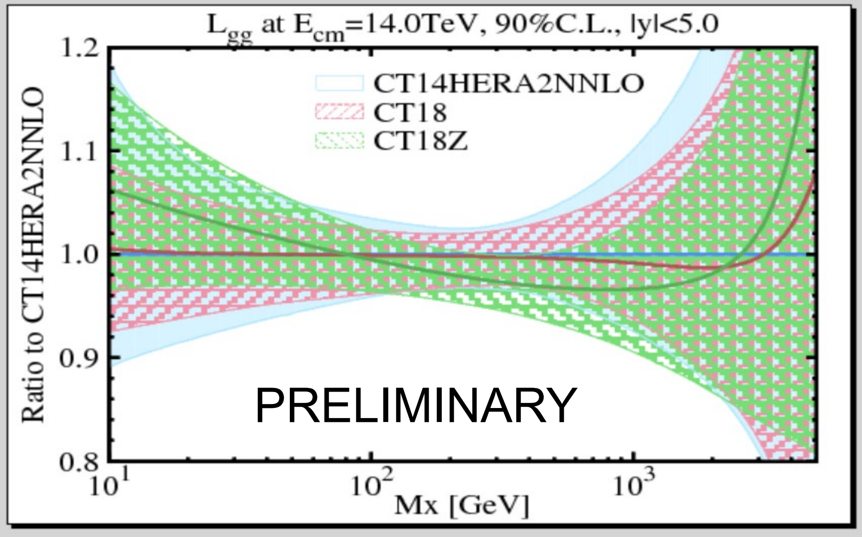

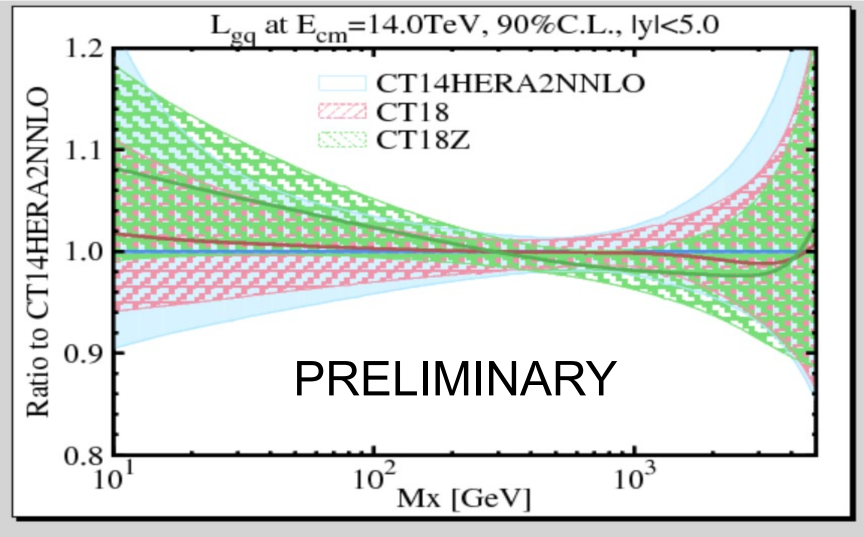

CT18 consistent with CT14

CT18Z has a somewhat different shape, especially at low invariant masses M_X

Mild reduction in nominal PDF error bands and cross section uncertainties

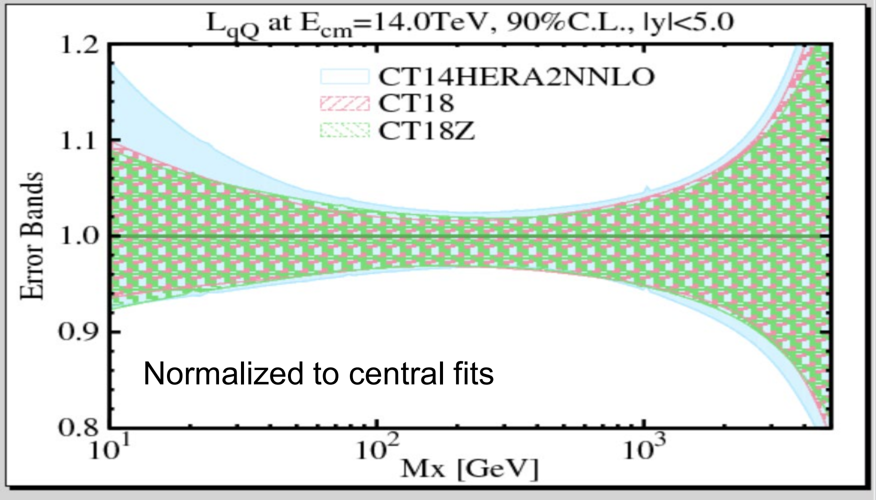

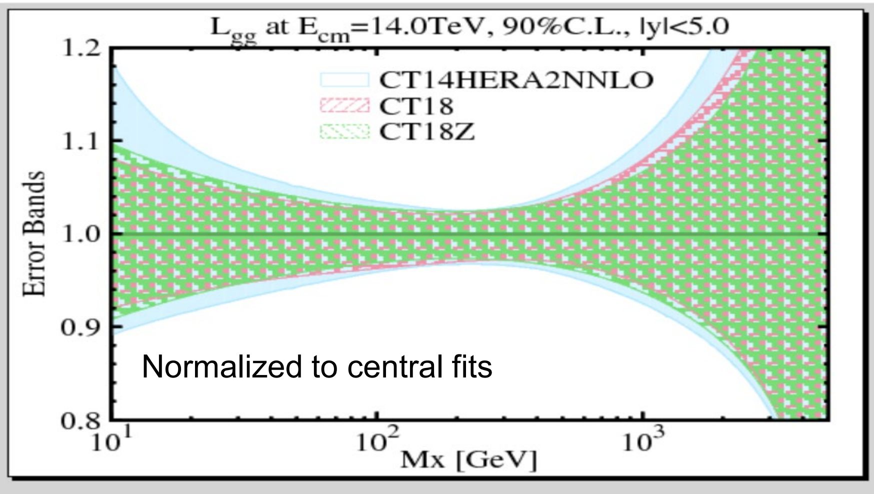

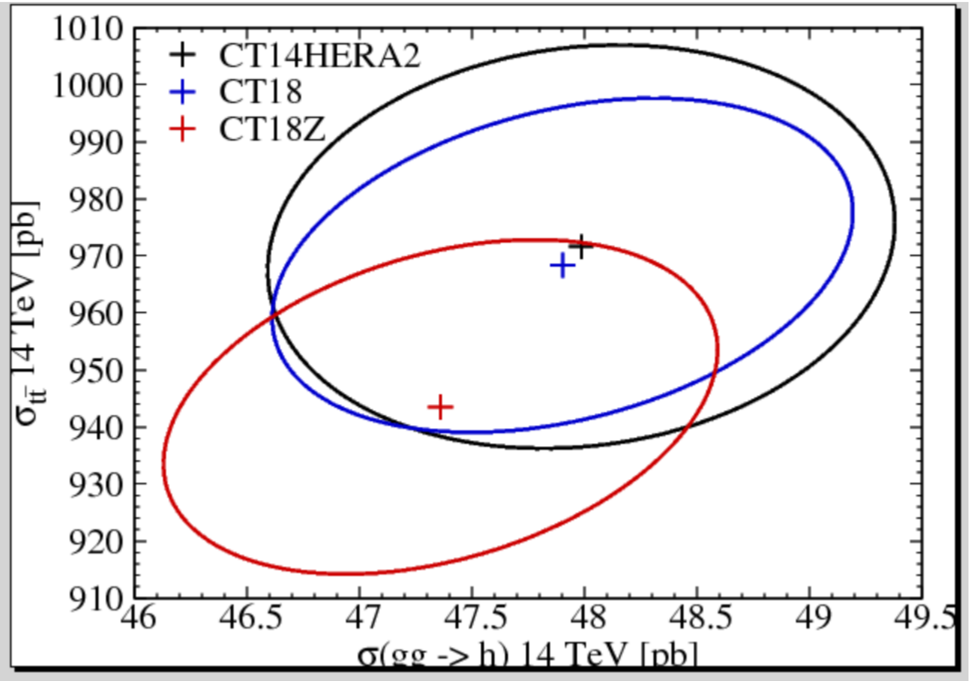

PRELIMINARY

CT18 in a nutshell

- Start with CT14-HERA2 (HERAI+II combined data released after publication of CT14)
- Examine a wide range of PDF parameterizations
- Use as much relevant LHC data as possible using applgrid/fastNLO interfaces to data sets, with NNLO/NLO K-factors, or fastNNLO tables in the case of top pair production. **Benchmark the predictions!**
- Examine **QCD scale dependence** in key processes
- Implement **parallelization** of the global PDF fitting to allow for faster turn-around time
- Validate the results using a **strong set of goodness-of-fit tests** *(Kovarik, PN, Soper,* arXiv:1905.06957*)*
- Use diverse statistical techniques (**PDFSense, ePump, Gaussian variables, Lagrange Multiplier scans**) to examine agreement between experiments

The questions we ask:

Which of 30+ eligible LHC experiments provide promising constraints on the CTEQ-TEA PDFs?

Do the LHC experiments agree among themselves and with other experiments?

The questions we ask:

Which of 30+ eligible LHC experiments provide promising constraints on the CTEQ-TEA PDFs?

Do the LHC experiments agree among themselves and with other experiments?

We elucidate these questions with a powerful combination of four methods:

1. **PDFSense and L_2 sensitivity** ⇒ Tim Hobbs, Tuesday and Wednesday
2. **ePump** ⇒ Carl Schmidt, Tuesday
1. **Effective Gaussian variables**
2. **Lagrange multiplier scans**

Experimental data in CT18 PDF analysis

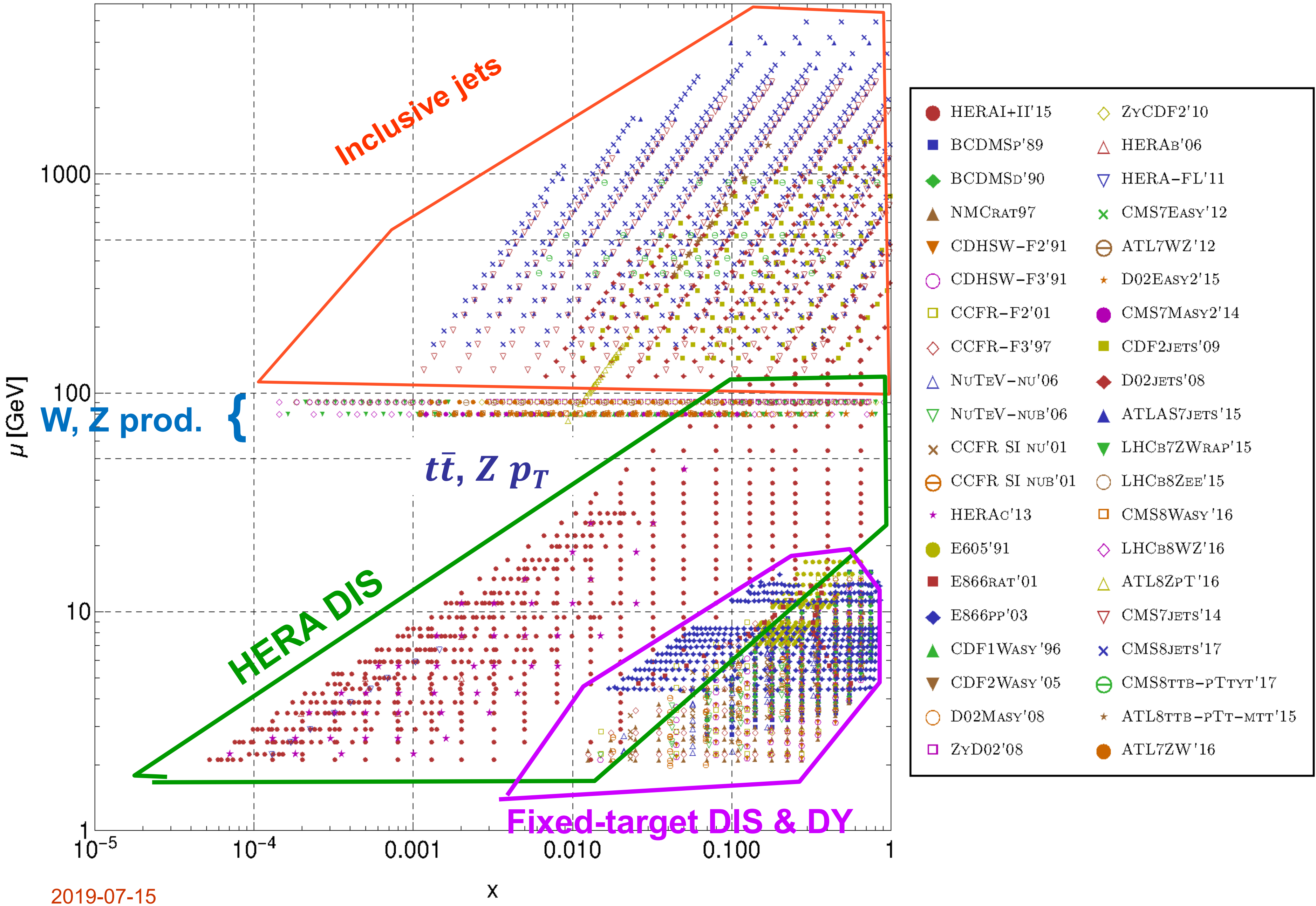

CT18(Z), χ^2 values

ID#	Experimental data set	$N_{pt,n}$	χ^2_n	$\chi^2_n/N_{pt,n}$	S_n
160	HERAI+II 1 fb^{-1}, H1 and ZEUS NC and CC $e^{\pm}p$ reduced cross sec. comb. [32]	1120	1405.1(1370.2)	1.25(1.22)	5.6(5.0)
101	BCDMS F_2^p [33]	337	376.3(385.8)	1.12(1.14)	1.5(1.8)
102	BCDMS F_2^d [34]	250	288.3(289.3)	1.15(1.16)	1.7(1.7)
104	NMC F_2^d/F_2^p [35]	123	123.3(114.5)	1.00(0.93)	0.061(-0.51)
108	CDHSW† F_2^p [36]	85	85.1	1.00	0.061
109	CDHSW† F_3^p [36]	96	83.1	0.865	-0.93
110	CCFR F_2^p [37]	69	78.3(74.6)	1.13(1.08)	0.81(0.52)
111	CCFR xF_3^p [38]	86	33.7(29.5)	0.391(0.343)	-5.3(-5.9)
124	NuTeV $\nu\mu\mu$ SIDIS [39]	38	19.3(29.7)	0.508(0.781)	-2.6(-0.96)
125	NuTeV $\bar{\nu}\mu\mu$ SIDIS [39]	33	36.5(54.7)	1.11(1.66)	0.50(2.3)
126	CCFR $\nu\mu\mu$ SIDIS [40]	40	29.2(33.0)	0.729(0.825)	-1.3(-0.76)
127	CCFR $\bar{\nu}\mu\mu$ SIDIS [40]	38	20.1(20.8)	0.530(0.550)	-2.4(-2.3)
145	H1 σ_r^b [41]	10	6.8(7.1)	0.682(0.710)	-0.65(-0.57)
147	Combined HERA charm production [42]	47	58.6(54.7)	1.25(1.16)	1.2(0.82)
169	H1 F_L [43]	9	17.1(14.5)	1.90(1.61)	1.7(1.2)
201	E605 Drell-Yan process [44]	119	100.3(98.0)	0.843(0.824)	-1.2(-1.4)
203	E866 Drell-Yan process $\sigma_{pd}/(2\sigma_{pp})$ [45]	15	10.0(12.2)	0.670(0.813)	-0.90(-0.43)
204	E866 Drell-Yan process $Q^3 d^2\sigma_{pp}/(dQdx_F)$ [46]	184	240.2(239.3)	1.31(1.30)	2.7(2.7)
225	CDF Run-1 electron A_{ch}, $p_{T\ell} > 25$ GeV [47]	11	9.1(9.2)	0.828(0.835)	-0.28(-0.27)
227	CDF Run-2 electron A_{ch}, $p_{T\ell} > 25$ GeV [48]	11	13.6(13.3)	1.23(1.21)	0.65(0.61)
234	DØ Run-2 muon A_{ch}, $p_{T\ell} > 20$ GeV [49]	9	9.3(9.2)	1.04(1.02)	0.23(0.19)
260	DØ Run-2 Z rapidity [50]	28	17.0(19.0)	0.606(0.680)	-1.6(-1.3)
261	CDF Run-2 Z rapidity [51]	29	49.6(62.6)	1.71(2.16)	2.3(3.4)
266	CMS 7 TeV 4.7 fb^{-1}, muon A_{ch}, $p_{T\ell} > 35$ GeV [52]	11	8.6(13.5)	0.785(1.23)	-0.40(0.64)
267	CMS 7 TeV 840 pb^{-1}, electron A_{ch}, $p_{T\ell} > 35$ GeV [53]	11	12.2(16.8)	1.11(1.53)	0.39(1.2)
268	ATLAS 7 TeV 35 pb^{-1} W/Z cross sec., A_{ch} [54]	41	44.1	1.08	0.41
281	DØ Run-2 9.7 fb^{-1} electron A_{ch}, $p_{T\ell} > 25$ GeV [55]	13	24.4(20.8)	1.88(1.60)	1.9(1.4)
504	CDF Run-2 inclusive jet production [56]	72	109.9(107.6)	1.53(1.49)	2.8(2.6)
514	DØ Run-2 inclusive jet production [57]	110	114.4(115.9)	1.04(1.05)	0.33(0.43)
245	LHCb 7 TeV 1.0 fb^{-1} W/Z forward rapidity cross sec. [23]	33	50.8(41.4)	1.54(1.25)	2.0(1.0)
246	LHCb 8 TeV 2.0 fb^{-1} $Z \to e^- e^+$ forward rapidity cross. sec. [24]	17	23.4(21.1)	1.37(1.24)	1.1(0.8)
248	ATLAS‡ 7 TeV 4.6 fb^{-1}, W/Z combined cross sec. [16]	34	(80.2)	(2.36)	(4.2)
249	CMS 8 TeV 18.8 fb^{-1} W cross sec. and A_{ch} [22]	11	10.8(11.0)	0.98(0.99)	0.09(0.1)
250	LHCb 8 TeV 2.0fb^{-1} W/Z cross sec. [25]	34	70.2(58.3)	2.07(1.71)	3.5(2.5)
251	ATLAS 8 TeV 20.3 fb^{-1} single diff. high-mass cross sec. [58]	12	18.7(?)	1.56(?)	1.3(?)
253	ATLAS 8 TeV 20.3 fb^{-1}, Z p_T cross sec. [27]	27	31.4(29.4)	1.16(1.09)	0.7(0.4)
542	CMS 7 TeV 5 fb^{-1}, single incl. jet cross sec., $R = 0.7$ (extended in y) [59]	158	208.7(204.24)	1.32(1.29)	2.6(2.4)
544	ATLAS 7 TeV 4.5 fb^{-1}, single incl. jet cross sec., $R = 0.6$ [60]	140	204.6(205.2)	1.46(1.47)	3.4(3.5)
545	CMS 8 TeV 19.7 fb^{-1}, single incl. jet cross sec., $R = 0.7$, (extended in y) [61]	185	249.4(229.1)	1.35(1.24)	3.1(2.2)
573	CMS 8 TeV 19.7 fb^{-1}, $t\bar{t}$ norm. double-diff. top p_T & y cross sec. [62]	16	30.4(26.3)	1.90(1.64)	2.1(1.6)
580	ATLAS 8 TeV 20.3^{-1}, $t\bar{t}$ p_T^t and $m_{t\bar{t}}$ abs. spectrum [63]	15	15.4(20.5)	1.03(1.36)	0.2(1.0)

Data sets employed in the CT18(Z) analysis. The numbers in round brackets are for the CT18Z fit. $N_{pt,n}$, χ^2 are the number of points and value of χ^2 for the n-th experiment at the global minimum. S_n is the effective Gaussian parameter quantifying agreement with each experiment.

1. New LHC datasets for CT18

1. 245 1505.07024 LHCb Z (W) muon rapidity at 7 TeV(applgrid)
2. 246 1503.00963 LHCb 8 TeV Z rapidity (applgrid);
3. 249 1603.01803 CMS W lepton asymmetry at 8 TeV (applgrid)
4. 250 1511.08039 LHCb Z (W) muon rapidity at 8 TeV(applgrid)
5. 253 1512.02192 ATLAS 7 TeV Z pT (applgrid)
6. 542 1406.0324 CMS incl. jet at 7 TeV with R=0.7 (fastNLO)
7. 544 1410.8857 ATLAS incl. jet at 7 TeV with R=0.6 (applgrid)
8. 545 1609.05331 CMS incl. jet at 8 TeV with R=0.7 (fastNLO)
9. 565 1511.04716 ATLAS 8 TeV tT pT diff. distributions (fastNNLO)
10. 567 1511.04716 ATLAS 8 TeV tT mtT diff. distributions (fastNNLO)
11. 573 1703.01630 CMS 8 TeV tT (pT , yt) double diff. distributions (fastNNLO)

12. 248 1612.03016 ATLAS 7 TeV Z and W rapidity (applgrid)->CT18Z
- also uses a special small-x factorization scale, charm mass m_c=1.4 GeV
- serious changes in PDFs, so warrants a separate PDF

PDFSense program: fast surveys of QCD data using a vector data technique

Estimates the sensitivity variable S_f ("correlation 2.0"): an easy-to-compute indicator of data point sensitivity to PDFs in the presence of experimental errors

References

1. **Mapping the sensitivity of hadronic experiments to nucleon structure**
B.-T. Wang, T.J. Hobbs, S. Doyle, J. Gao, T.-J. Hou, P. M. Nadolsky, F. I. Olness
Phys.Rev. D98 (2018) 094030

2. **The coming synergy between lattice QCD and high-energy phenomenology**
T.J. Hobbs, Bo-Ting Wang, Pavel Nadolsky, Fredrick Olness
arXiv:1904.00222

3. **PDFSense: Mapping the PDF sensitivity of HL-LHC, LHeC, and EIC**
T.J. Hobbs, Bo-Ting Wang, Pavel Nadolsky, Fredrick Olness
arXiv:1907.00988

Sensitivity of hadronic experiments to PDFs

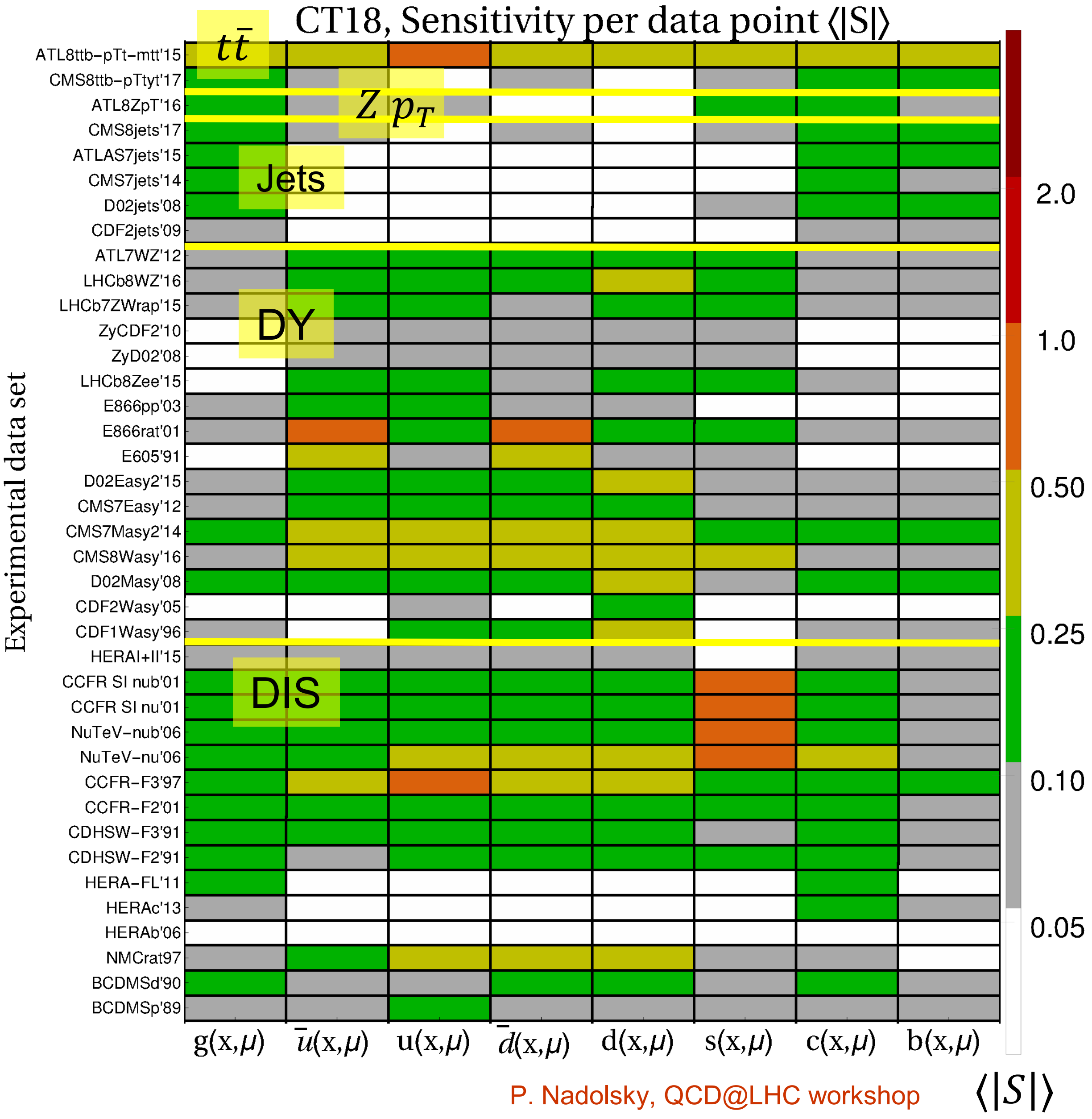

Computed using the **PDFSense** method **[arXiv:0803.02777]**

Average sensitivity to $f_a(x_i, \mu_i)$ **per data point**

- defined in the backup
- expt. and PDF errors included

Red bars = most sensitive experiments

Sensitivity of hadronic experiments to PDFs

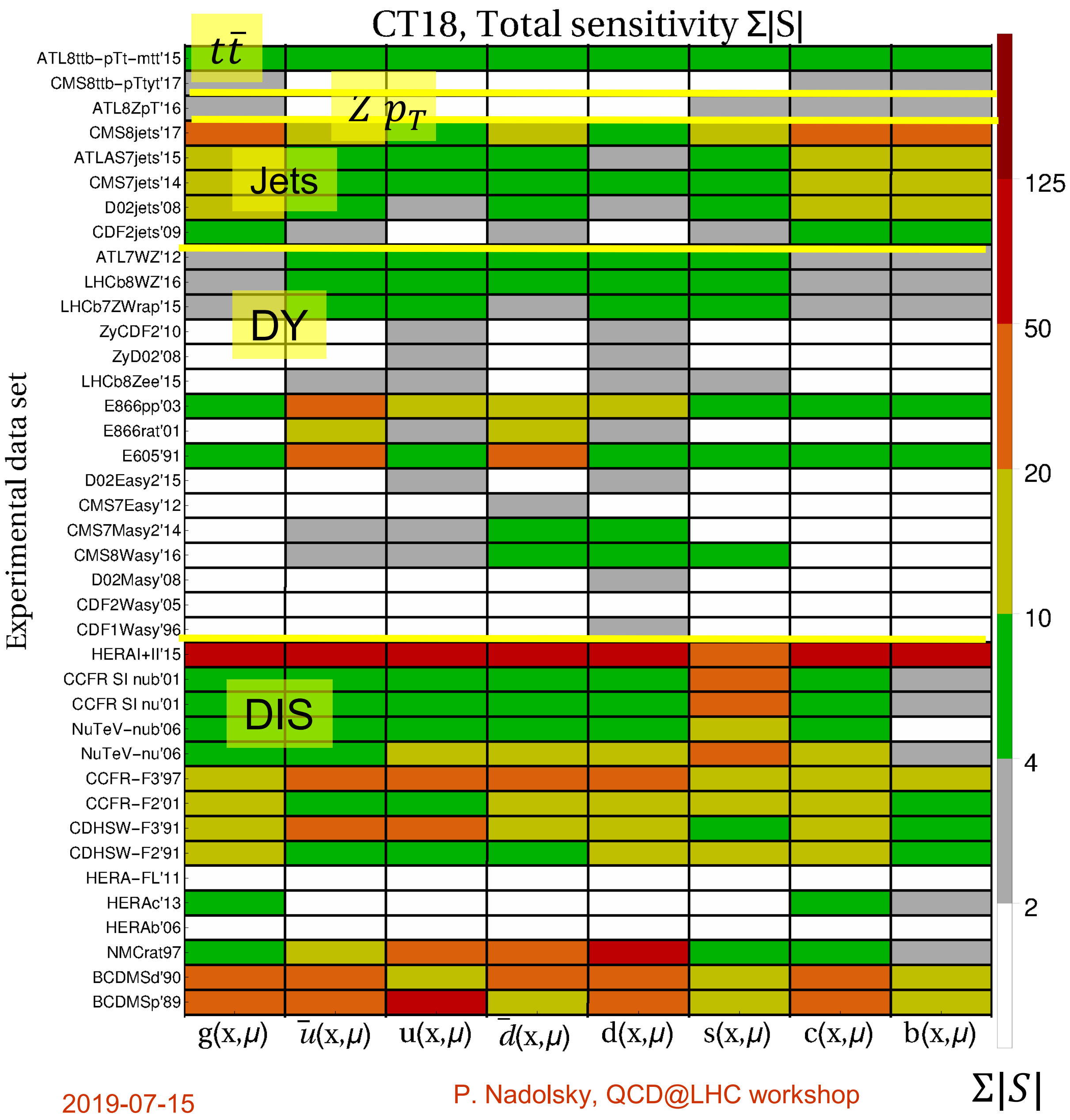

Total sensitivity to $f_a(x_i, \mu_i)$, **summed over data points**

$$\sum_{points} |S_{f,i}|$$

Computed using the **PDFSense** code
[arXiv:0803.02777]

Sensitivity of hadronic experiments to PDFs

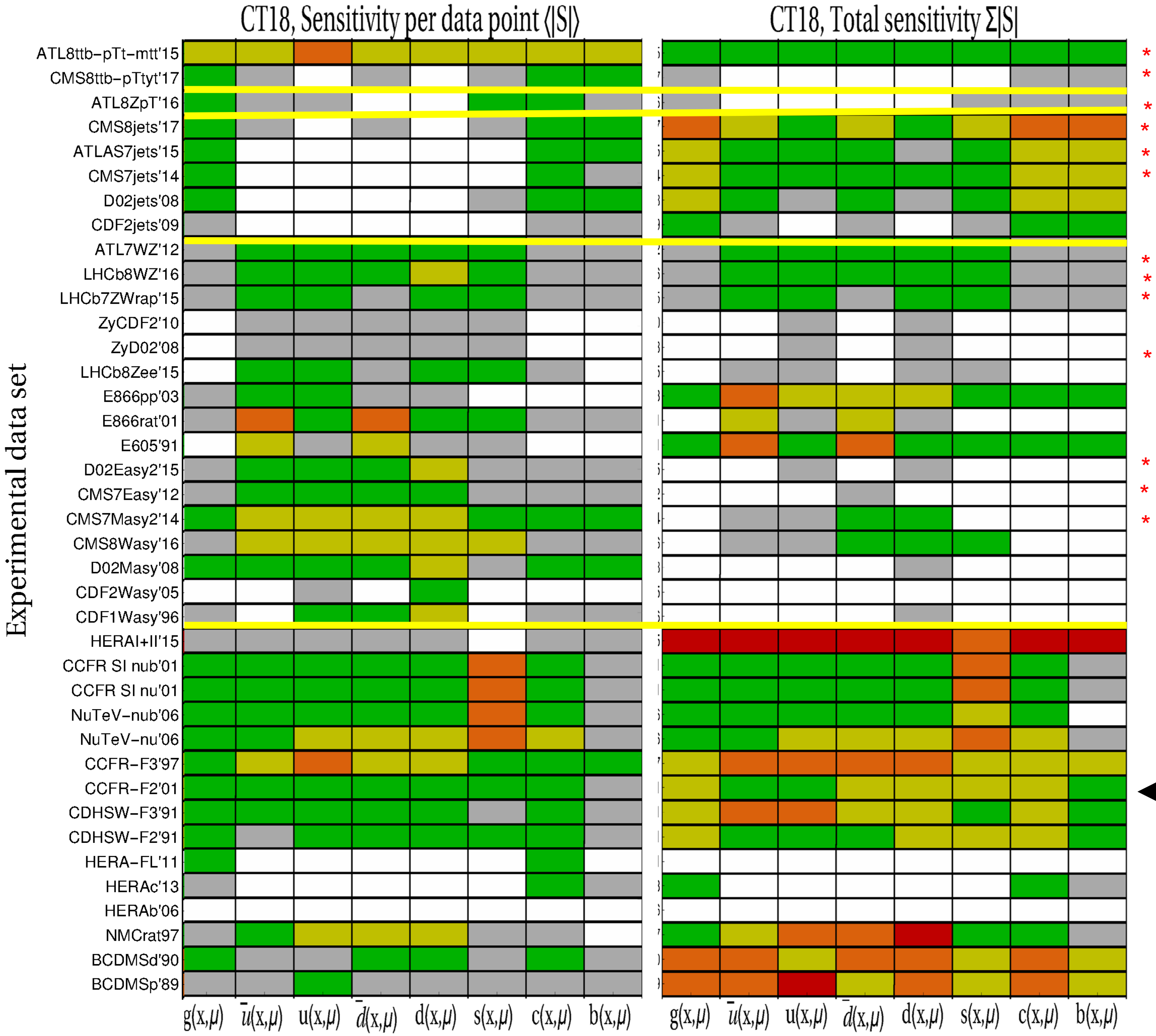

The LHC data sets (*) hold a great promise – if they agree

HERA I+II, BCDMS, NMC, DIS data sets dominate experimental constraints. Large numbers of data points matter!

Sensitivity of hadronic experiments to PDFs

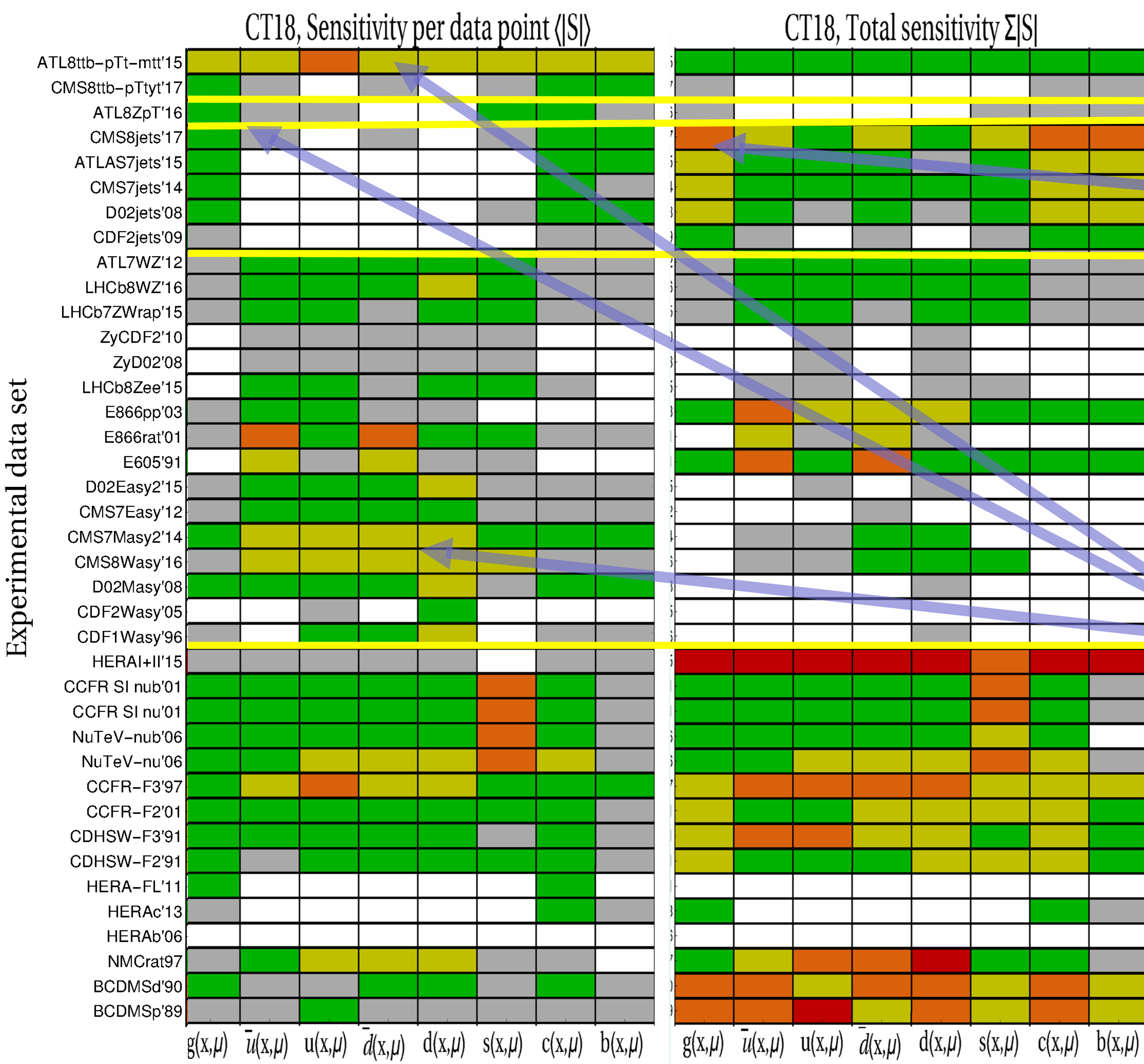

CMS 7 & 8 TeV single-inclusive jet production has highest total sensitivity ($N_{pt} > 100$), modest sensitivity per data point

$t\bar{t}$, CMS W asy, high-p_T Z production have high sensitivity per data point, smaller total sensitivity ($N_{pt} \sim 10-20$)

Are the global QCD data sets mutually compatible?

Not quite. ☹

Effective Gaussian variables

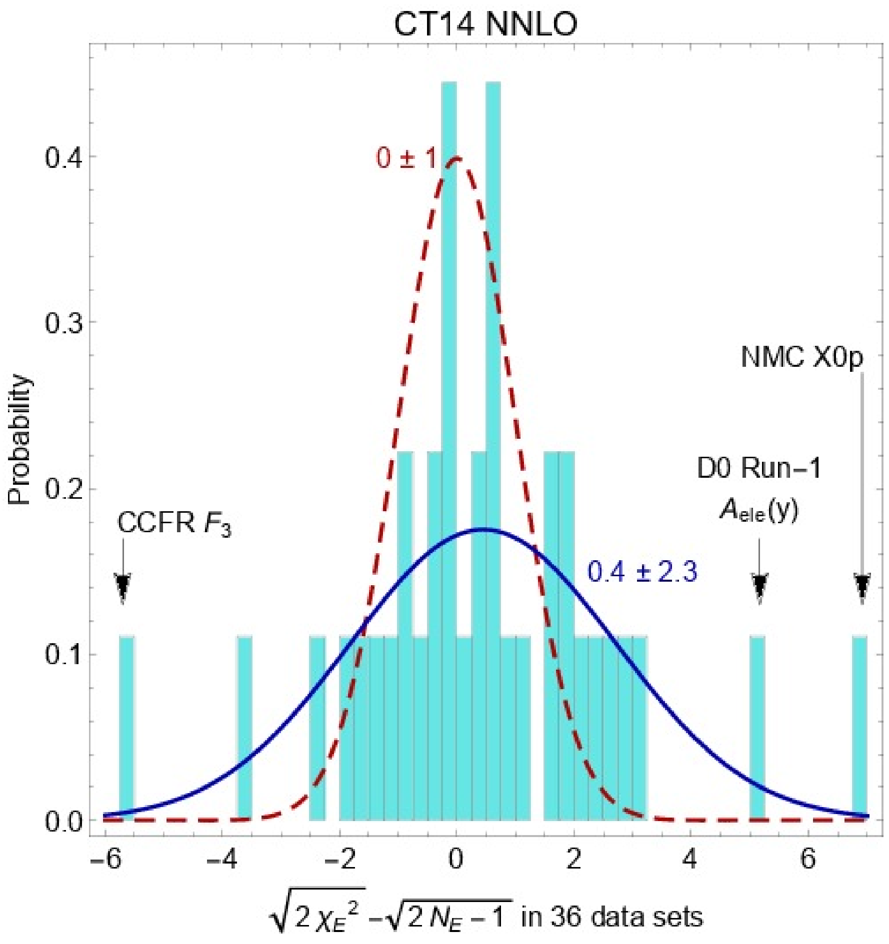

Define $S_n(\chi^2, N_{pt})$ for experiment n so that, in a perfect fit, it would approximately obey the standard normal distribution $\mathcal{N}(0,1)$ (mean=0, half-width=1) independently of $N_{pt,n}$

[H.-L. Lai et al., arXiv:1007.2241; S.Dulat et al., arXiv:1309.0025; K. Kovarik, P.N., D. Soper, arXiv:1905.06957]

Effective Gaussian variables

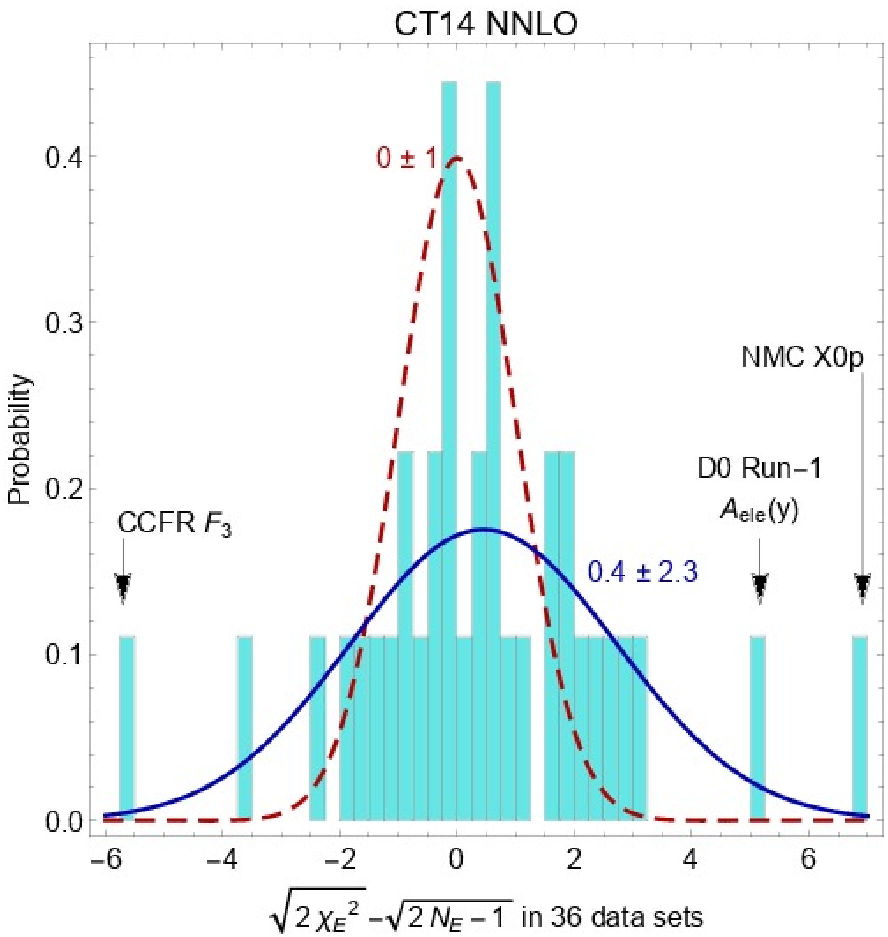

$$S_n(\chi^2, N_{pt}) \equiv \sqrt{2\chi^2} - \sqrt{2N_{pt} - 1}$$

$S_n(\chi_n^2, N_{pt,n})$ are Gaussian distributed with mean 0 and variance 1 for $N_{pt,n} \geq 10$ **[R.A.Fisher, 1925]**

Even more accurate (χ^2, N_{pt}): **T.Lewis, 1988**

An empirical S_n distribution can be compared to $\mathcal{N}(0,1)$ visually or using a statistical (Anderson-Darling, Kolmogorov-Smirnov, …) test

Effective Gaussian variables

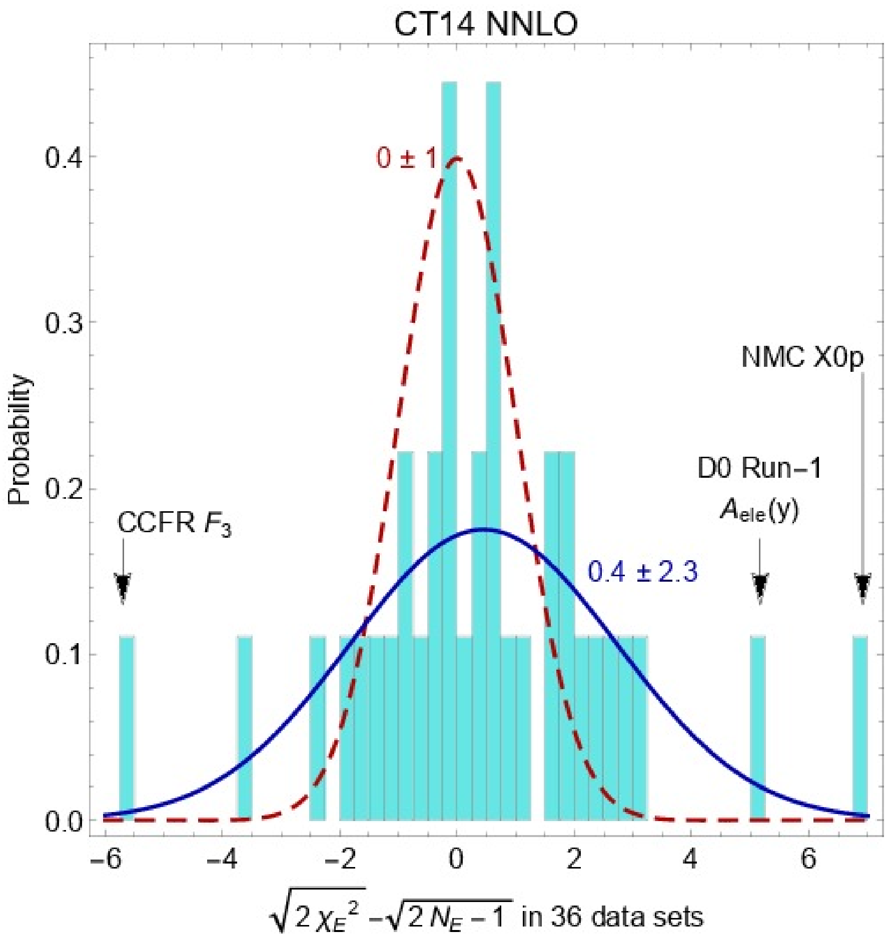

Some S_n are too big or too small in a global fit

CT14 NNLO:

- $S_n > 4$ for NMC DIS ep cross section and D0 Run-1 electron charge asymmetry
- These data sets are eliminated in CT14HERA2/CT18 fits
- The rest of CT14 experiments are reasonably consistent; $S_n \sim \mathcal{N}(0.3, 1.6)$

- Qualitatively similar S_n distributions for MMHT, NNPDF3.X

CT18 (CT18Z) NNLO

13 (14) new LHC experiments with 665 (711) data points

- New LHC experiments tend to have larger S_n
- ATLAS 7 TeV Z, W production has $S_n \approx 5.2$, included in CT18Z fit only

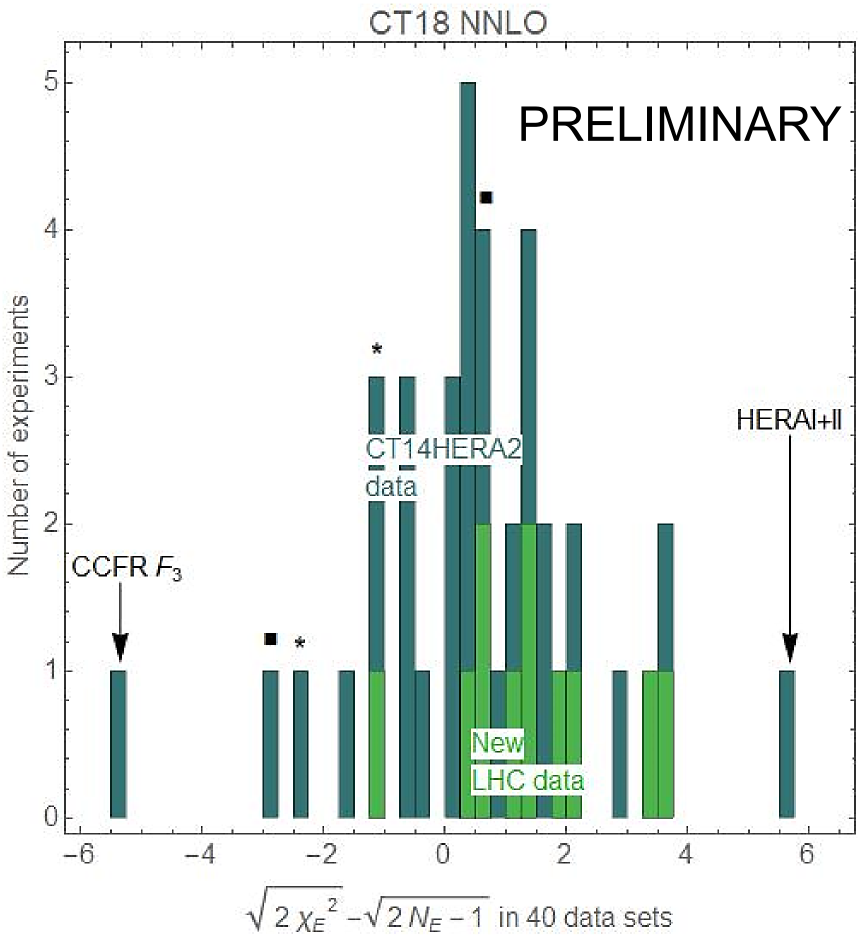

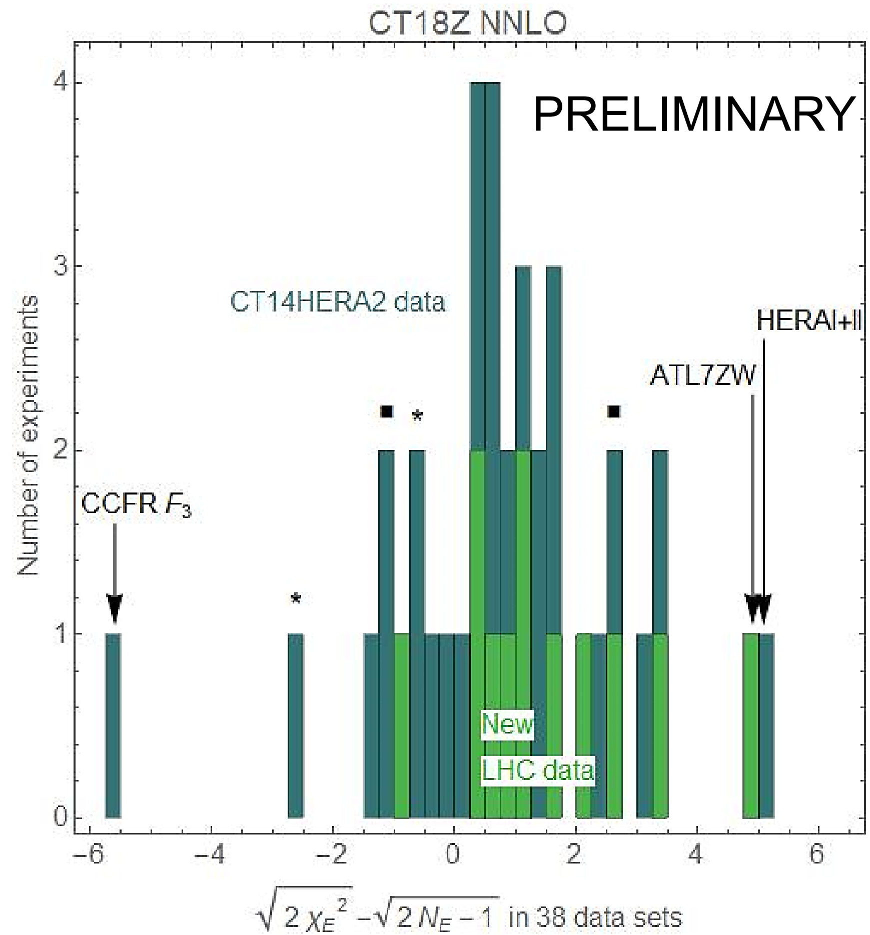

CT14 PDFs with HERA1+2 (=HERA2) combination

Phys.Rev. D95 (2017) 034003

Separate the four HERA2 DIS processes;
(Q_{cut} = 2 GeV)

	N_{pts}	$\chi^2_{red.}$ / N_{pts}
NC e^+p	880	1.11
CC e^+p	39	1.10
NC e^-p	159	1.45
CC e^-p	42	1.52
totals		
[reduced χ^2] /N	1120	1.17
χ^2 / N	1120	1.25
R^2 / N	1120	0.08

e^+p data are fitted fine

e^-p data are fitted poorly

reduced χ^2 values

χ^2 = [reduced χ^2] + R^2

The quadratic penalty for 162 systematic errors = 87.5

Fair (not perfect) agreement; can be mildly improved by the QCD scale choice

CT18X and Z: a special factorization scale in DIS

The CT18Z fits uses a $\mu_{DIS,X}$ scale that reproduces many features of NNLO-NLLx fits with $\ln(1/x)$ resummation by the NNPDF [arXiv:1710.05935] and xFitter [1802.0064] groups.

$$\mu_{DIS,X}^2 = 0.8^2 \left(Q^2 + \frac{0.3\ GeV^2}{x^{0.3}} \right)$$

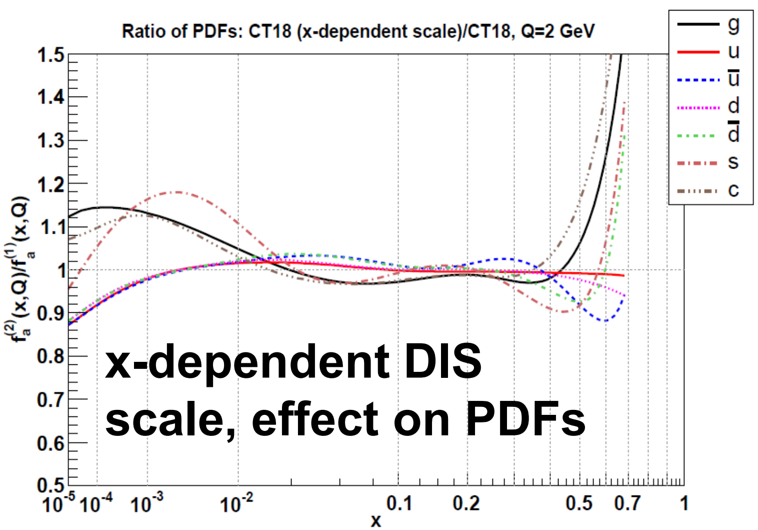

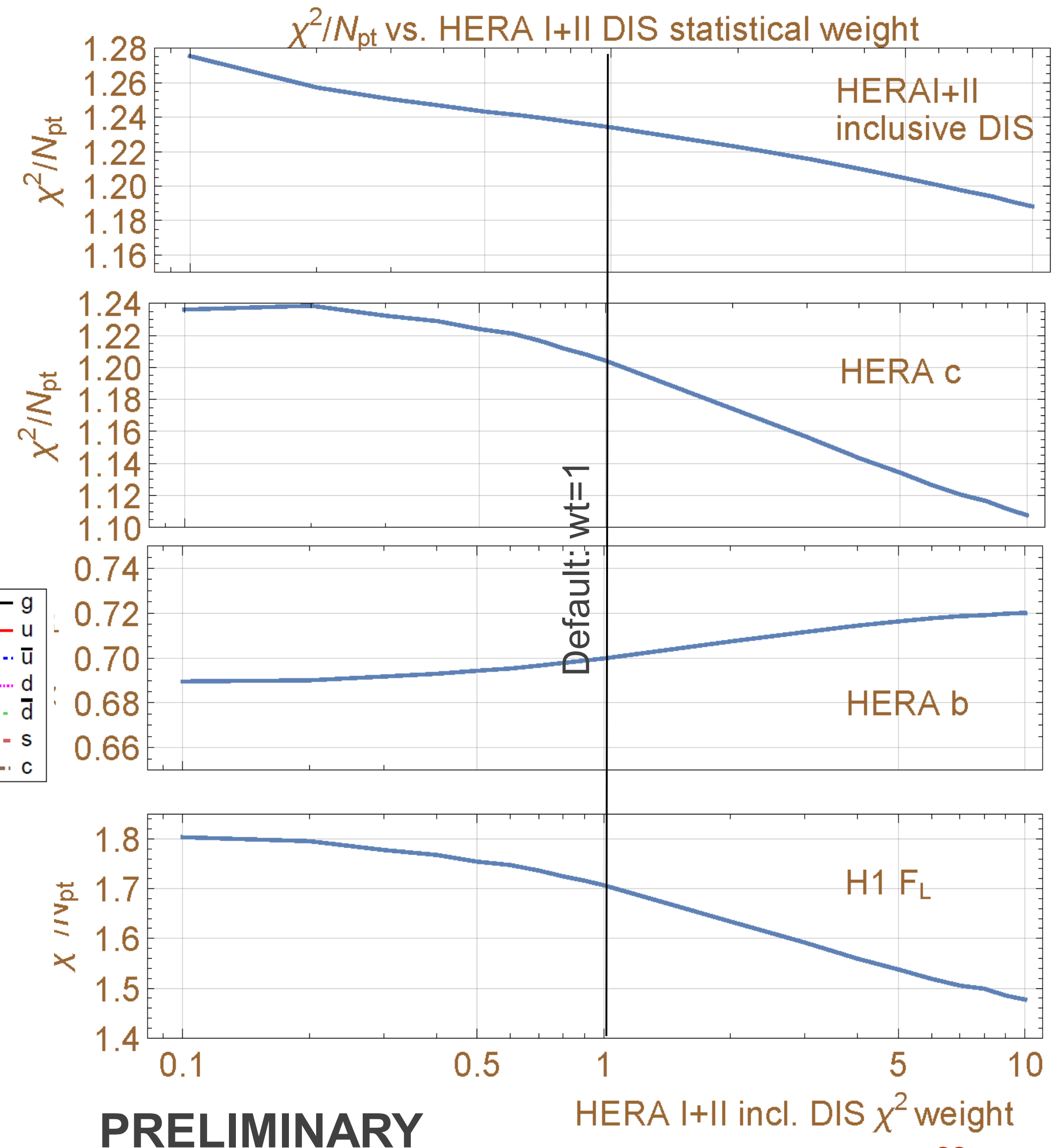

CT18X and Z: a special factorization scale in DIS

Right: when the χ^2 weight for the **inclusive** HERA I+II DIS is increased to $wt = 10$ to suppress pulls from the other experiments, χ^2_{CT18Z}/N_{pt} for HERA I+II DIS **and** HERA charm production decreases to about the same levels as in HERA-only NNLO+NLLx fits by other groups.

- **NNLO with an x-dependent scale is statistically indistinguishable from BFKL resummation in the CT18 x-Q region (Q > 2 GeV)**

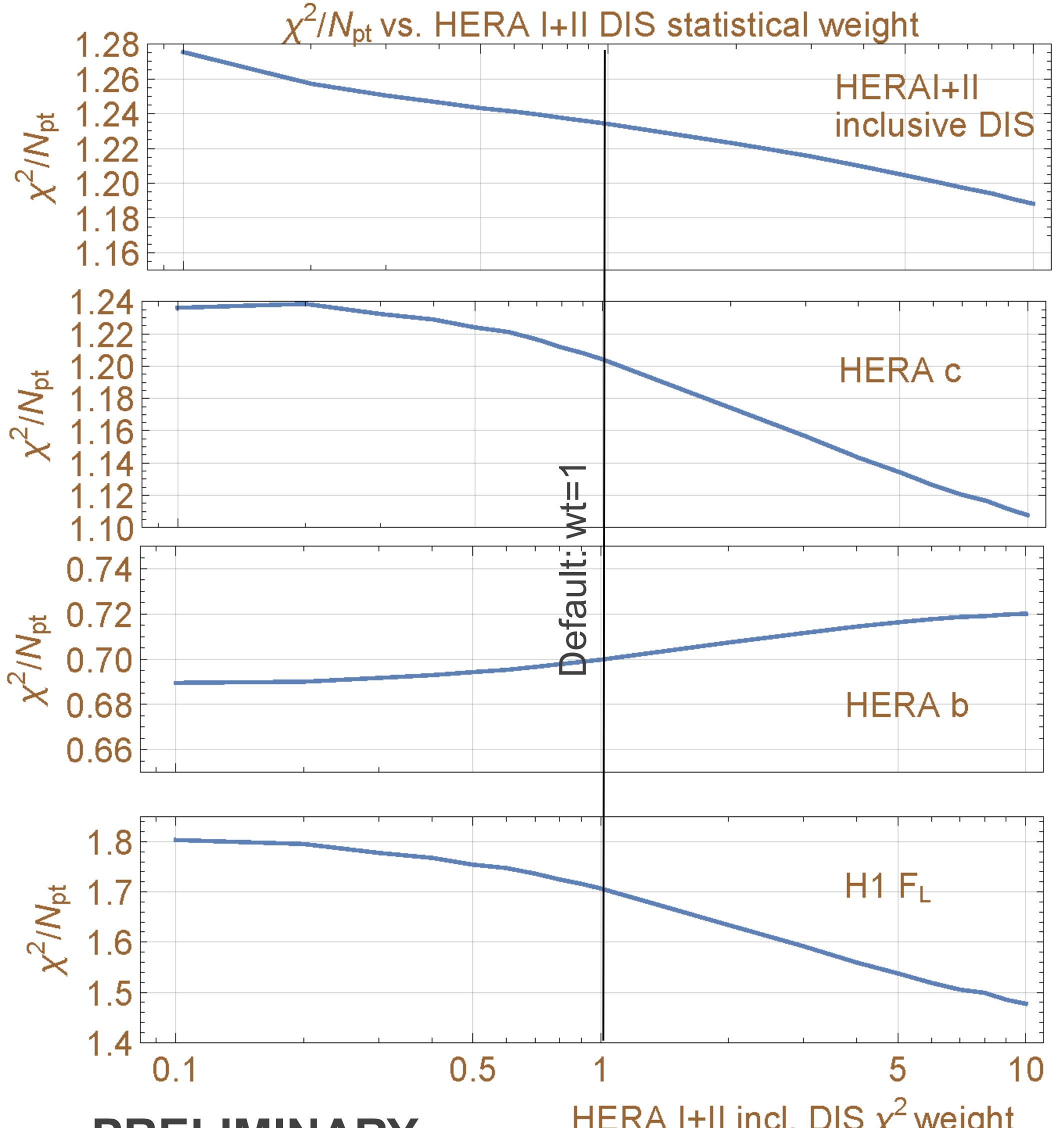

PRELIMINARY

Lagrange Multiplier (LM) Scans: $\alpha_s(M_Z)$

The LM scan technique is introduced in **Stump et al., Phys.Rev. D65 (2001) 014012**

☺ **Detailed dependence of χ^2** ☹ **slow; refitting on a supercomputing cluster**

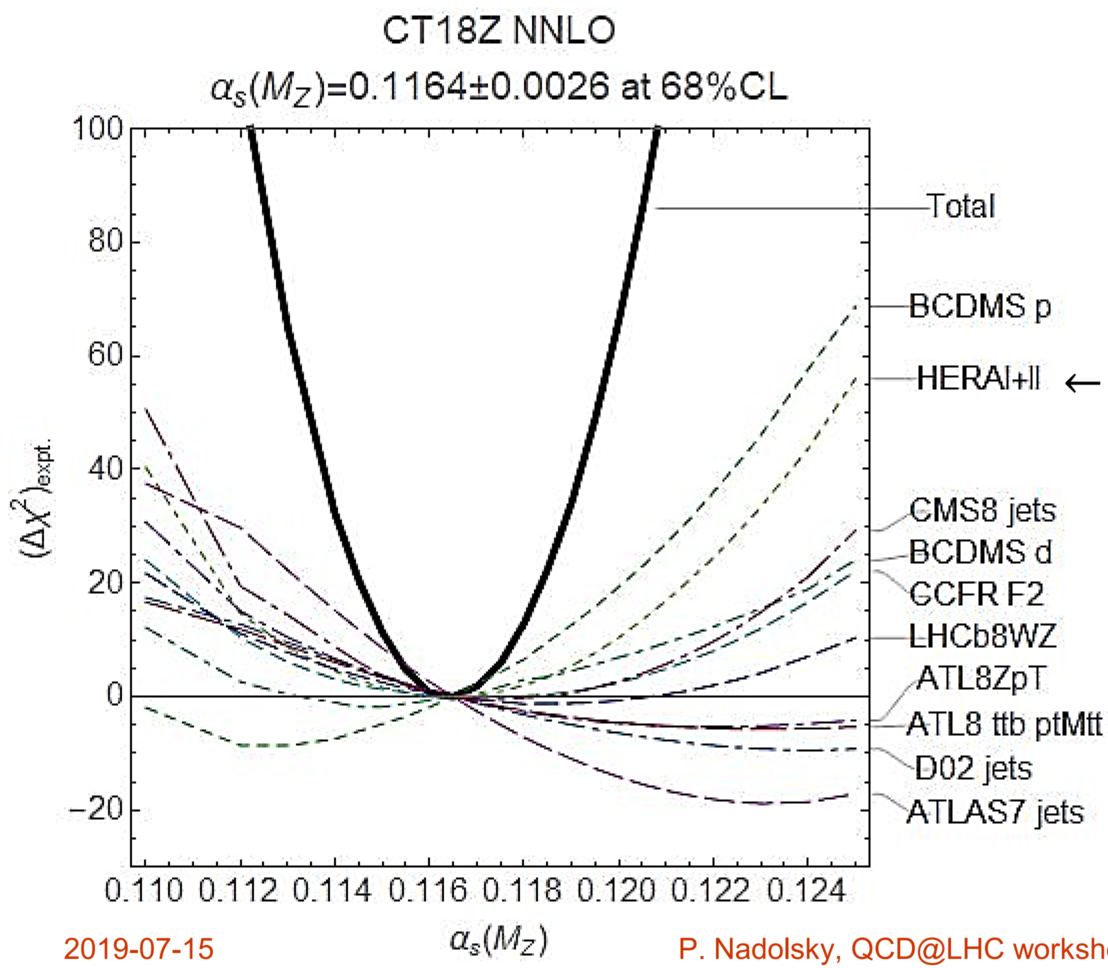

← flatter than in CT18

$\alpha_s(m_Z)$ from global fit closer to 0.117 than to 0.118

Lagrange Multiplier scan: $g(0.01, 125\ GeV)$

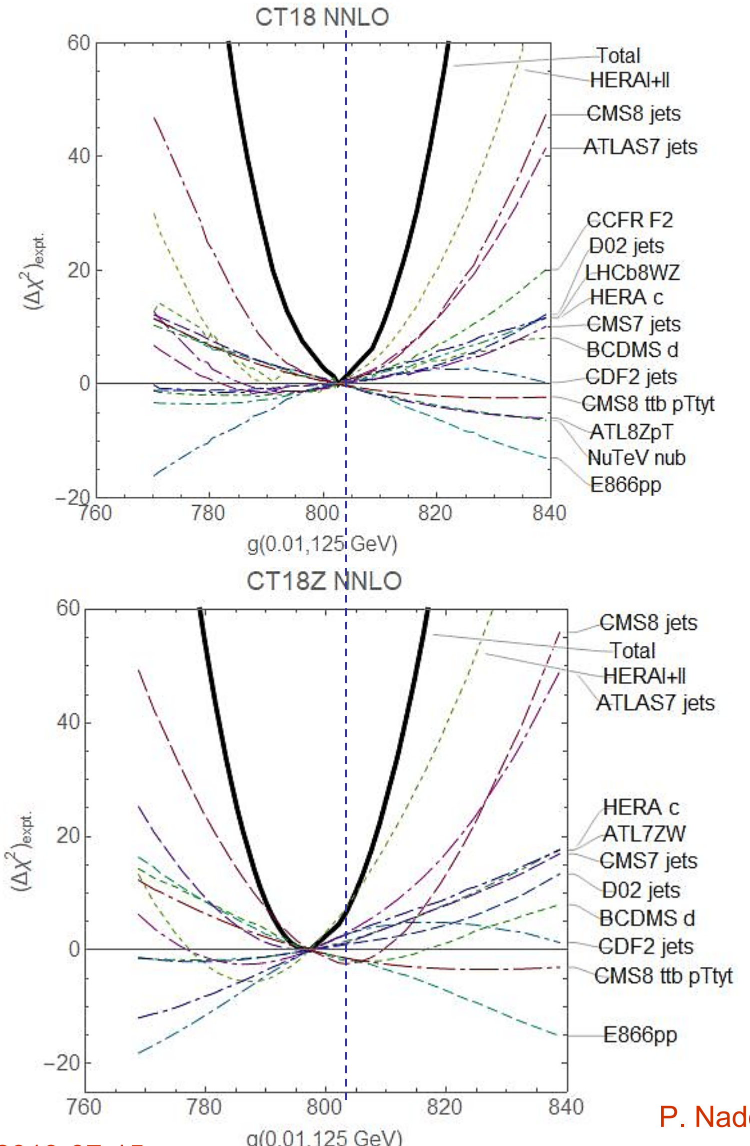

Upper row: CT18

- HERAI+II data set provides the dominant constraint, followed by ATLAS, CDF2, CMS, D02 jet production, HERA charm,…
- $t\bar{t}$ double-diff. cross sections provide weaker constraints

Lower row: CT18Z

- CT18Z: a 1% lower NNLO gluon in the Higgs production region than for CT14/CT18

Lagrange Multiplier scan: $g(0.3, 125\ GeV)$

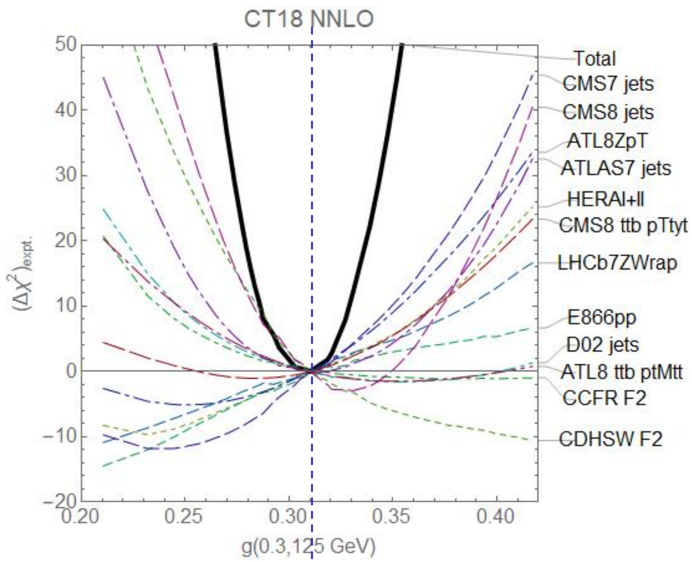

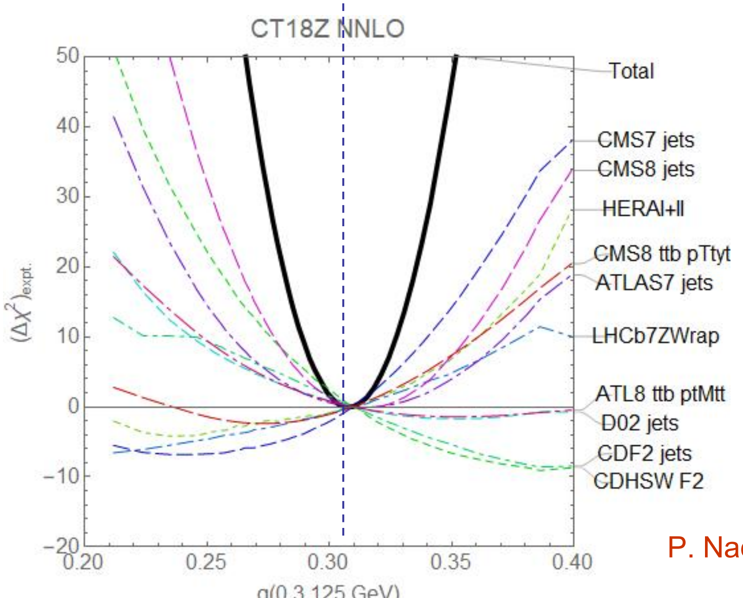

Upper/lower rows: CT18/CT18Z

Good overall agreement. But observe opposite pulls from ATLAS7/CMS7 jet production and CMS8 jet production

Similarly, ATLAS $t\bar{t}$ distributions $\mathrm{d}^2\sigma/(dp_{T,t}dm_{t\bar{t}})$ and CMS $t\bar{t}$ distributions $\mathrm{d}^2\sigma/(dp_{T,t}dy_{t,ave})$ at 8 TeV impose weak opposite pulls

Constraints from ATLAS 8 $Z\ p_T$ production data are moderate and still affected by NNLO scale uncertainty

LM scans on χ^2 weights of HERA I+II, ATLAS 7 Z/W, and NuTeV data

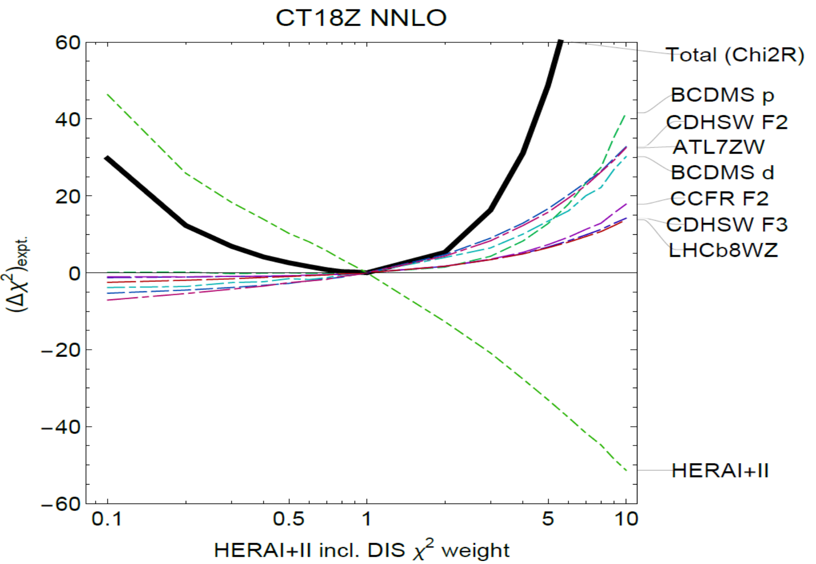

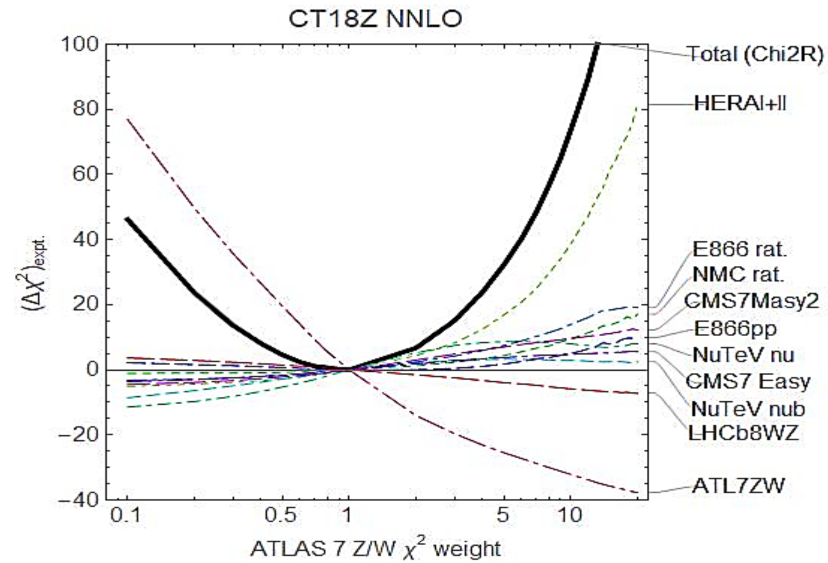

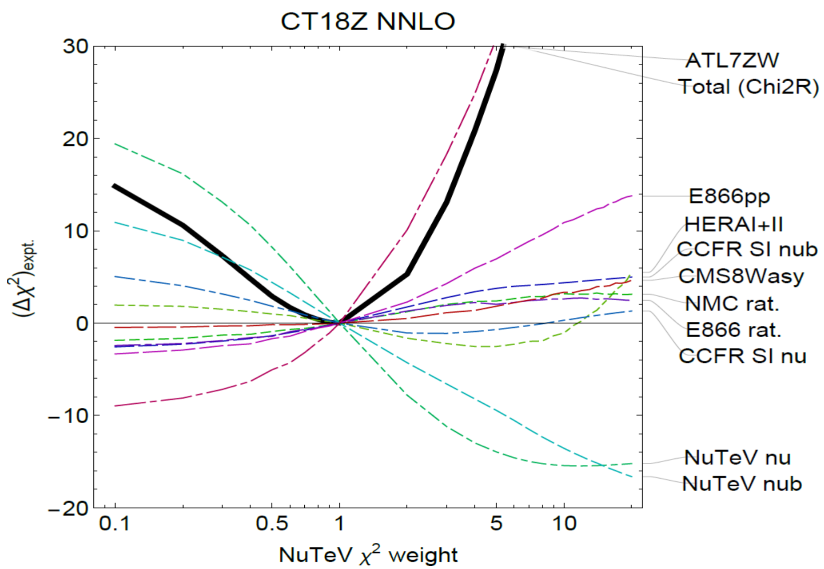

Fits with varied weights and LM scans reveal a disagreement between important DIS [primarily HERA, CCFR, NuTeV,…] and DY [primarily ATL7ZW, E866, LHCb8WZ,…] experiments. This is more pronounced for large$-x$ gluon as well as strangeness.

Lagrange Multiplier scan: $\mathrm{R}_s(x = 0.023, \mu = 1.5\ GeV)$

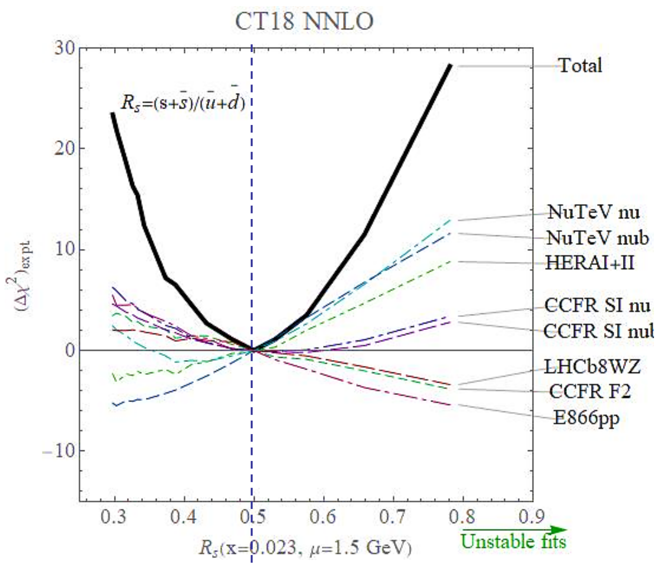

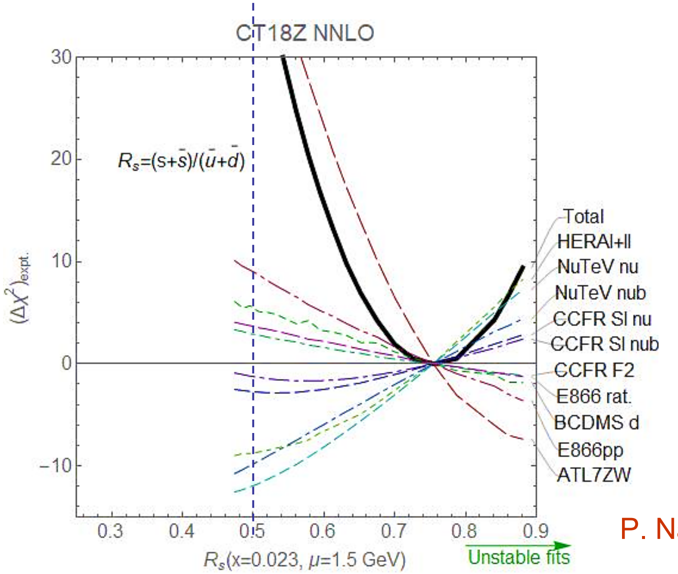

The CT18Z strangeness is increased primarily as a result of including the ATLAS 7 TeV W/Z production data (not in CT18), as well as because of using the DIS saturation scale and $m_c^{pole} = 1.4$ GeV

In either CT18 or CT18Z fit, observe instability in the fits for $R_s > 1$ at $x = 0.01 - 0.1$

Compare to

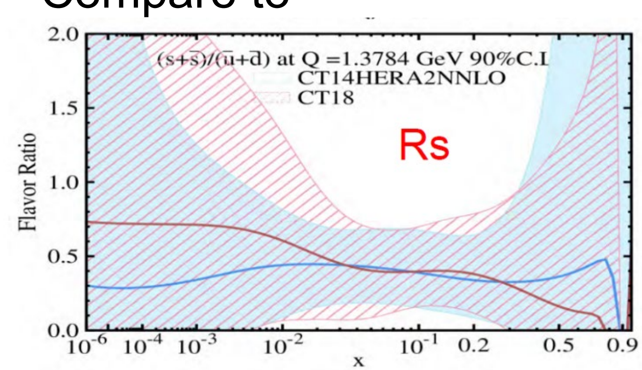

Effect on PDF uncertainties

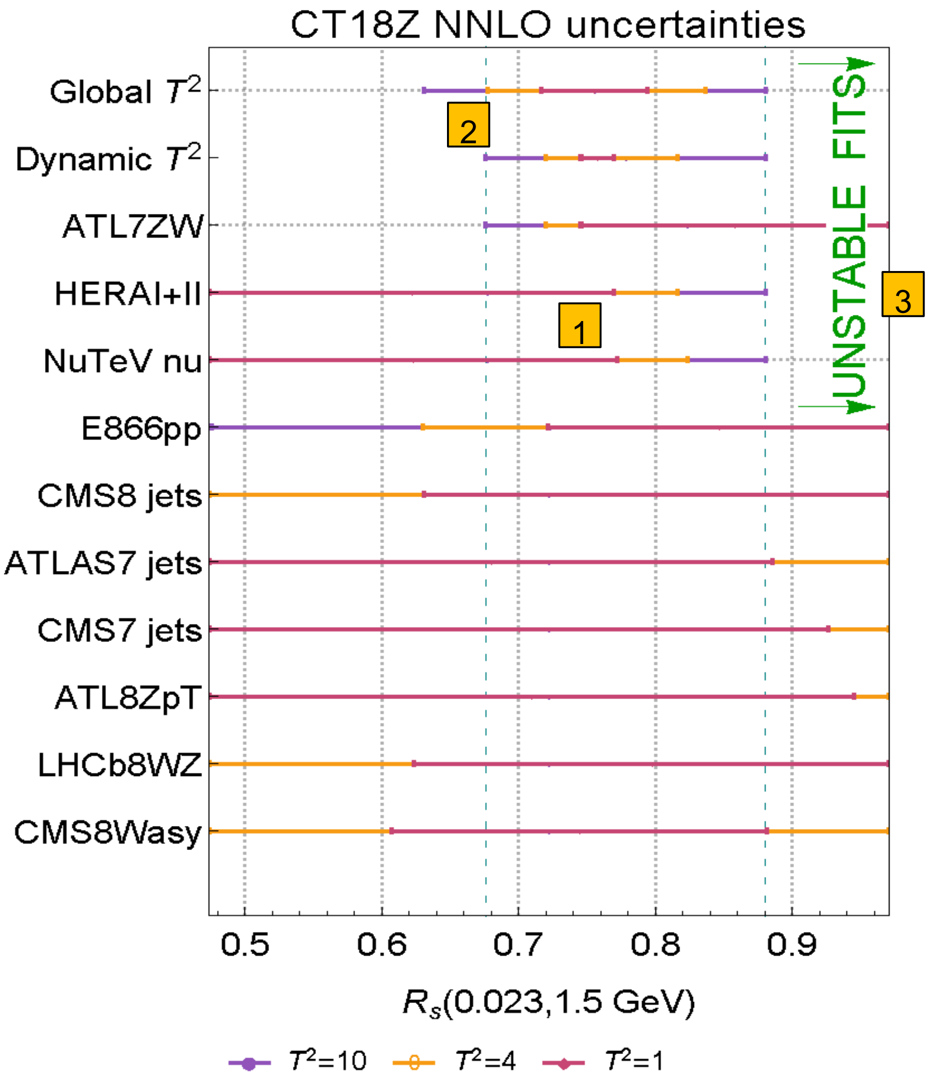

The LM scan reveals details not captured by other methods

1 **Nonlinearities:** the error bands for tolerance $T^2 = 1,4,10$ may not scale according to the Gaussian distribution

2 **Tensions:** in the affected direction(s), the global tolerance and **especially dynamic tolerance** may underestimate the true PDF error.

3 χ^2 **instability:** Neither the "global T^2" nor "dynamic T^2" reflect instability of fits at $R_s > 0.9$

Key points, the CT18(Z) global QCD analysis

- modest reduction in the PDF uncertainties compared to CT14
- DIS experiments dominate constraints on PDFs
- LHC Run-1 and 2 processes (jet, W/Z, high-p_T Z, $t\bar{t}$, $W+c$, …production) will provide promising constraints once they are brought into mutual agreement
- NNLO DIS cross sections with an x-dependent factorization scale behave like NNLO+NNLx resummed ones, are incorporated in CT18Z PDFs with the modified small-x gluon and strangeness
- **Future reduction of NNLO PDF uncertainties is not automatic. The goals of the HL-LHC program demand a broad coordinated effort to eliminate tensions between experimental measurements that were identified using several techniques (L_2 sensitivity, LM scans,…)**

Backup

Theory input

Obs.	Expt.	fast table	NLO code	K-factors	R,F scales
Inclusive jet	ATL 7 CMS 7/8	APPLgrid fastNLO	NLOJet++	NNLOJet	p_T, p_T^1
p_T^Z	ATL 8	APPLgrid	MCFM	NNLOJet	$\sqrt{Q^2 + p_{T,Z}^2}$
W/Z rapidity W asymmetry	LHCb 7/8 ATL 7 CMS 8	APPLgrid	MCFM/aMCfast	FEWZ/MCFM	$M_{W,Z}$
DY (low,high mass)	ATL 7/8 CMS 8	APPLgrid	MCFM/aMCfast	FEWZ/MCFM	Q_{ll}
$t\bar{t}$	ATL 8 CMS 8	fastNNLO			$\frac{H_T}{4}, \frac{m_T}{2}$

when justified, a small Monte-Carlo error (typically 0.5%) added for NNLO/NLO K-factors

Theory calculations must be benchmarked before the PDF4LHC'20 combination!

One program/scale not sufficient for understanding theory uncertainties

2019-07-15

Theoretical calculations for vector boson production

ID	Obs.	Expt.	fast table	NLO code	K-factors	$\mu_{R,F}$
245 246 250 249	$y_{\mu\mu}, \eta_\mu$ y_{ee} $y_{\mu\mu}, \eta_\mu$ $A(\mu)$	LHCb7ZW LHCb8Z LHC8ZW CMS8W	APPLgrid	MCFM/aMCfast	MCFM/FEWZ	$M_{Z,W}$
253	p_T^{ll}	ATL8Z	APPLgrid	MCFM	NNLOJet	M_T^{ll}
201 203 204	$\sqrt{\tau}, y$ $\sigma_{pd}/\sigma_{pp}, x_F$ Q, x_F	E605 E866 E866	CTEQ		FEWZ	Q_{ll}
225 227 234 281	A(e) A(e) $A(\mu)$ A(e)	CDF1Z CDF2W D02W D02W	CTEQ		ResBos	Q_{ll} M_W
260 261	y_{ll} y_{ll}	D02 CDF2	CTEQ		VRAP	Q_{ll}
266 267 268	$A(\mu)$ A(e) $y_{ll}, \eta_l, A(l)$	CMS7W CMS7W ATL7ZW(2012)	CTEQ		ResBos	M_W $M_{Z,W}$
248	y_{ll}, η_l	ATL7ZW(2016)	APPLgrid	MCFM/aMCfast	MCFM/FEWZ	$M_{Z,W}$

Fitting code parallelization with multi-threads

upgrade to a parallelized version of the fitting code, two-layer parallelization: 1. through rearrangement of the minimization algorithm; 2. via redistribution of the data sets

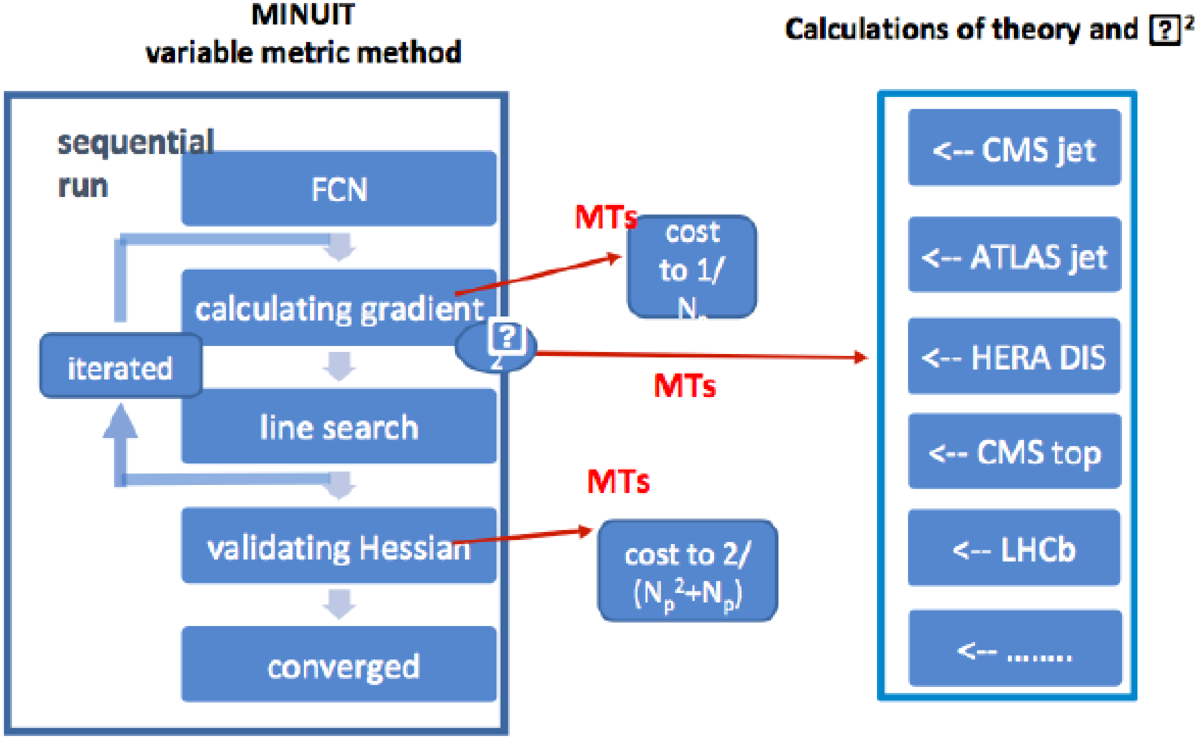

Layer 1: after all a factor of 4~5 improvement on speed is achieved!

Layer 2: further speed up by a factor of 2, depending on data sets included

Functional forms of PDFs

Evolving PDF models

- EW precision fits and PDF fits are fundamentally different.
  - In an EW fit ("ZFITTER program"), the Standard Model parameters are found by fitting a **fixed** theoretical model.
  - In a PDF fit ("XFITTER program"), the theoretical model (PDF parametrization) **evolves** when more data are added.

⇒ A PDF model can change its functional form within some limits to evade falsification by a new data set

- The uncertainty due to the PDF functional form contributes as much as 50% of the total PDF uncertainty in CT fits. The CT18 analysis estimates this uncertainty using 100 trial functional forms. This part of analysis requires significant human intervention.

Carefully crafted PDF functional forms with >20-30 free parameters

Explore various non-perturbative parametrization forms of PDFs

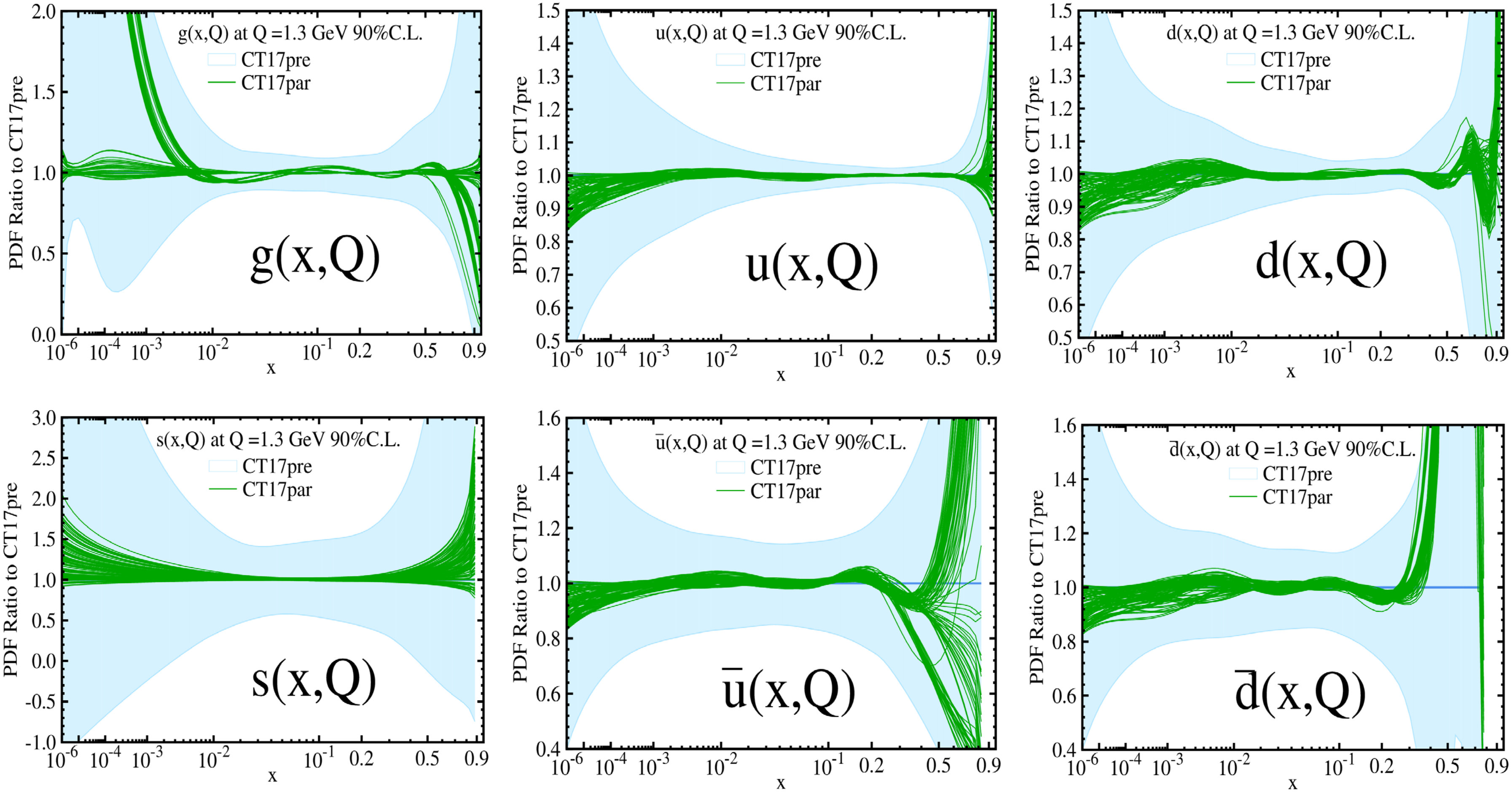

- CT17par – sample result of using various non-perturbative parametrization forms.
- No data constrain very large x or very small x regions.

CT14: parametrization forms

- CT14 relaxes restrictions on several PDF combinations that were enforced in CT10. [These combinations were not constrained by the pre-LHC data.]
  - The assumptions $\frac{\bar{d}(x,Q_0)}{\bar{u}(x,Q_0)} \to 1$, $u_v(x,Q_0) \sim d_v(x,Q_0) \propto x^{A_{1v}}$ with $A_{1v} \approx -\frac{1}{2}$ at $x < 10^{-3}$ are relaxed once LHC W/Z data are included
  - CT14 parametrization for $s(x,Q)$ includes extra parameters
- Candidate CT14 fits have 30-35 free parameters
- In general, $\mathrm{f_a}\,(\mathrm{x},\mathrm{Q_0}) = \mathrm{A}x^{a_1}(1-\mathrm{x})^{\mathrm{a_2}}\mathrm{P_a}(\mathrm{x})$
- CT10 assumed $P_a(x) = \exp(a_0 + a_3\sqrt{x} + a_4 x + a_5\, x^2)$
  - exponential form conveniently enforces positive definite behavior
  - but power law behaviors from a_1 and a_2 may not dominate
- In CT14, $\mathrm{P_a}(\mathrm{x}) = \mathrm{G_a}(\mathrm{x})\mathrm{F_a}(\mathrm{z})$, where $\mathrm{G_a}(\mathrm{x})$ is a smooth factor
  - $\mathrm{z} = 1 - 1(1-\sqrt{\mathrm{x}})^{\mathrm{a_3}}$ preserves desired Regge-like behavior at low x and high x (with $\mathrm{a_3}$>0)
- Express $F_a(z)$ as a linear combination of Bernstein polynomials:

$$z^4, 4z^3(1-z), 6z^2(1-z)^2\,, 4z(1-z)^3, (1-z)^4$$

  - each basis polynomial has a single peak, with peaks at different values of z; reduces correlations among parameters

If too few parameters

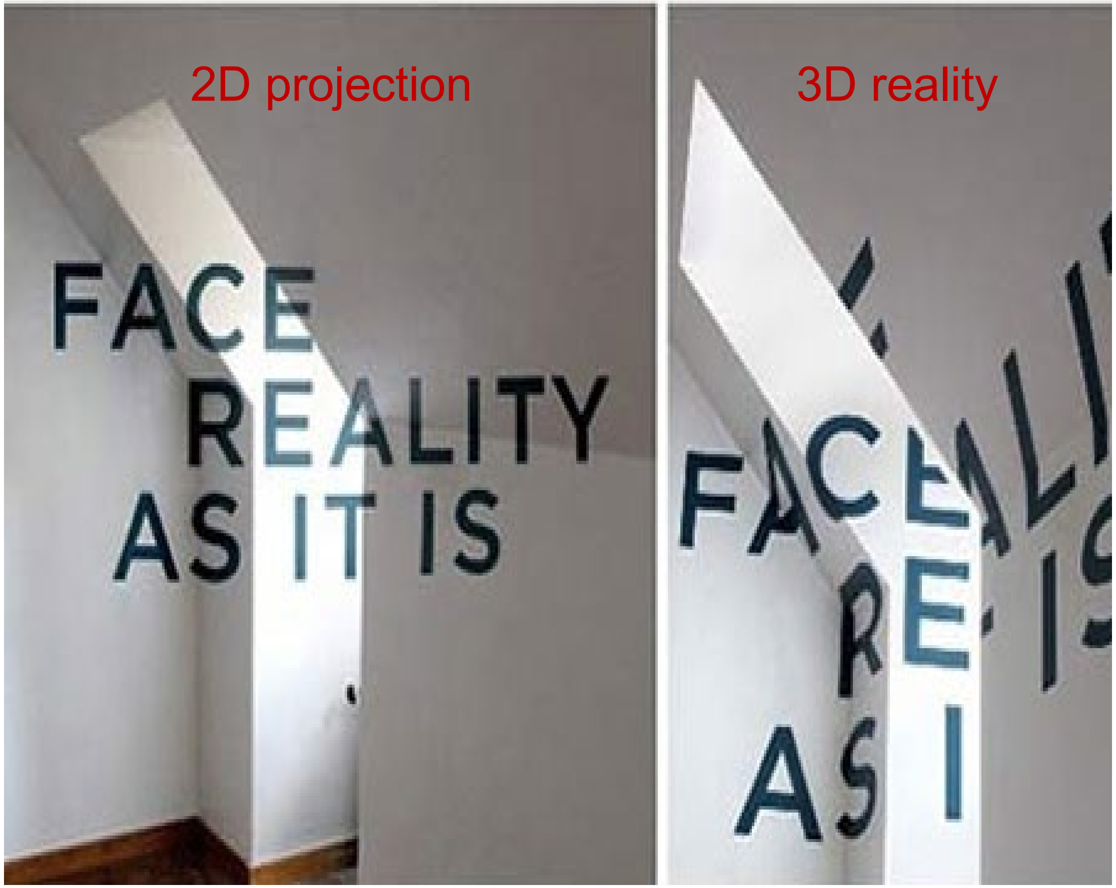

The solution can be consistent and false

If too many parameters

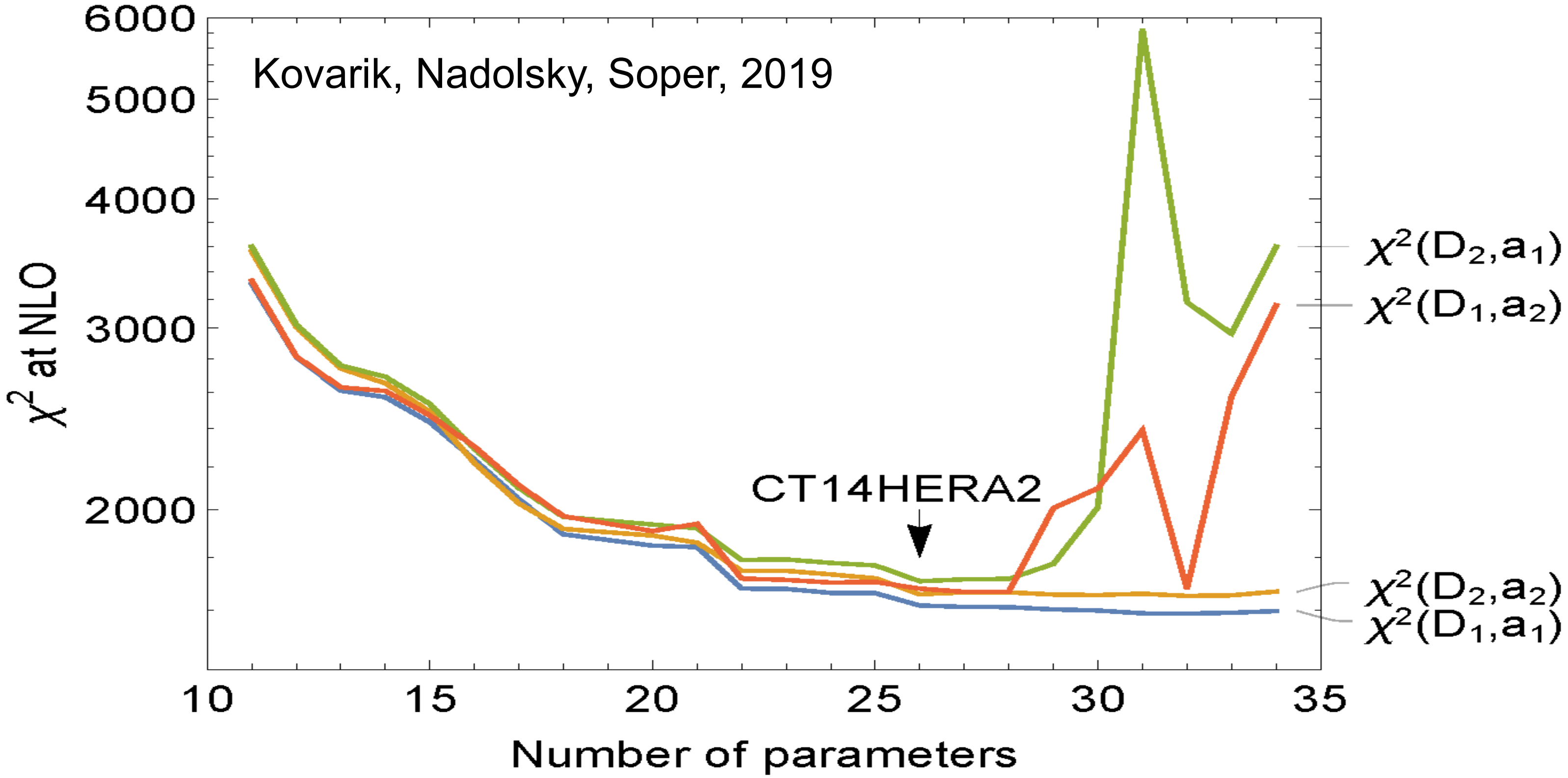

- Randomly split the CT14HERA data set into two halves, D_1 and D_2
- Find parameter vectors a_1 and a_2 from the best fits for D_1 and D_2, respectively

If too many parameters

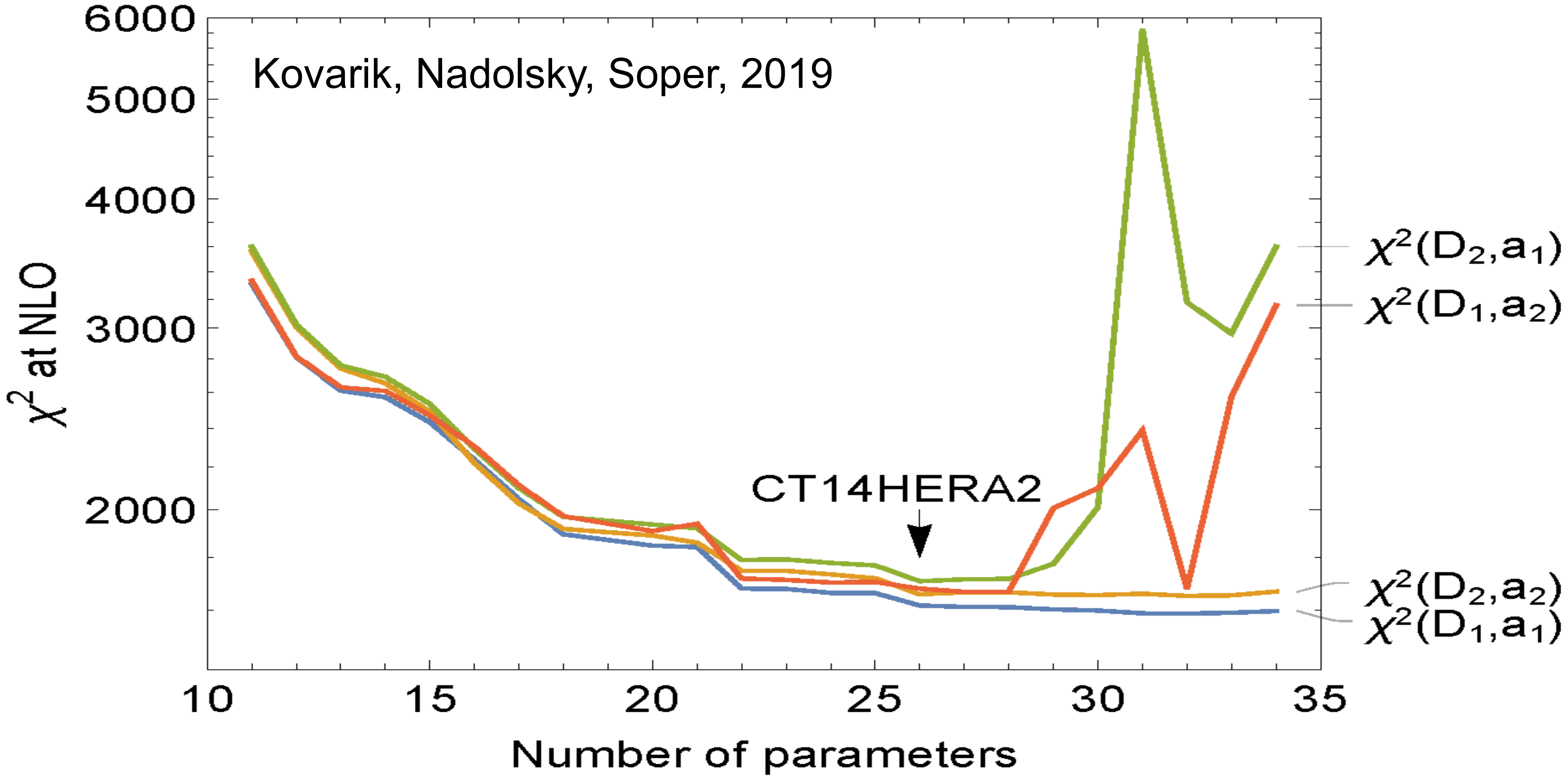

- **Fitted samples:** $\chi^2(D_1, a_1)$ and $\chi^2(D_2, a_2)$ uniformly decrease with the number of parameters
- **Control samples:** $\chi^2(D_2, a_1)$ and $\chi^2(D_1, a_2)$ fluctuate when the number of parameters is larger than about 30

If too many parameters

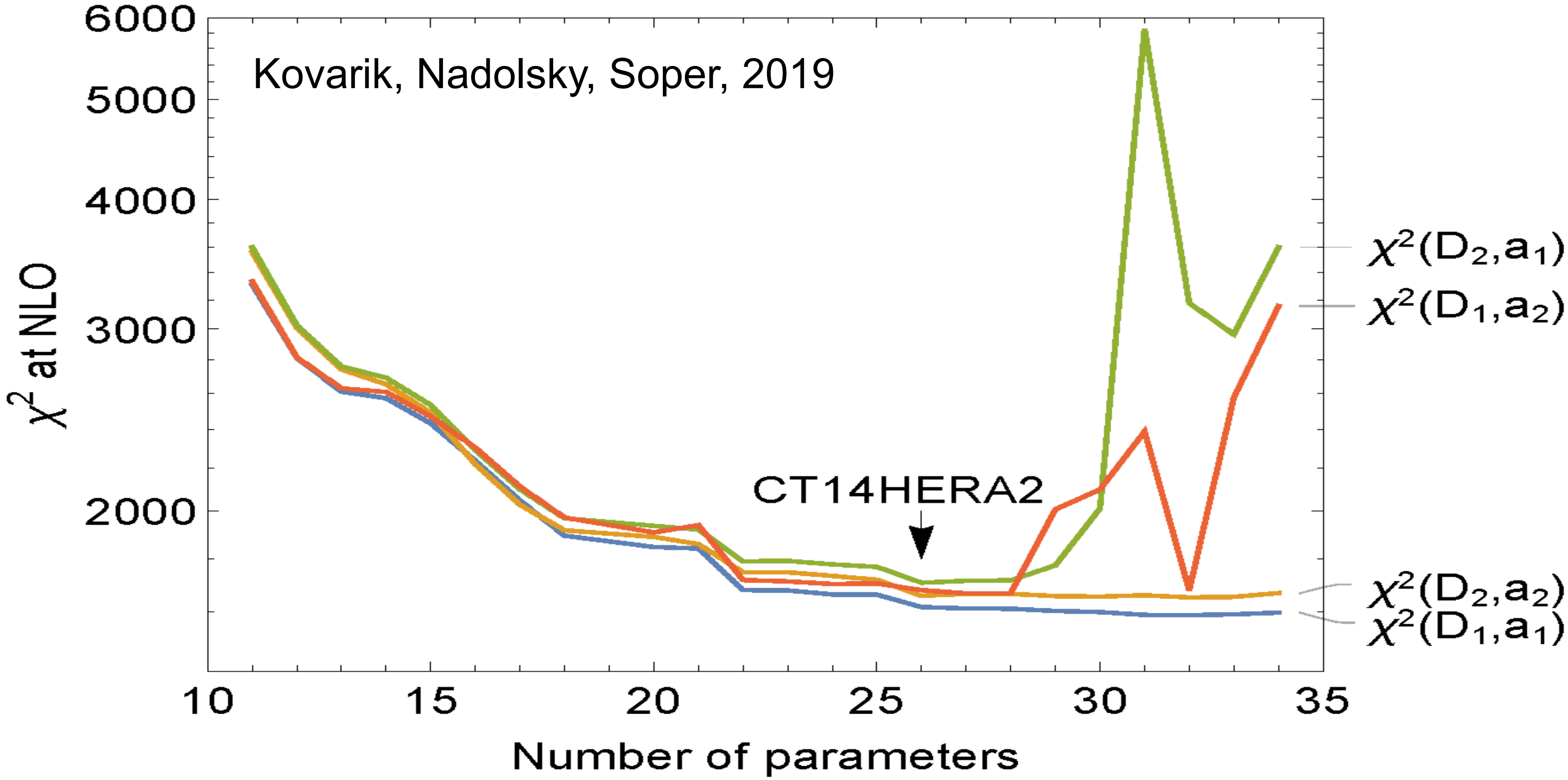

$\lesssim 30$ parameters (26 in CT14HERA2) is optimal for describing the CT14HERA2 data set

Vectors of data point residuals…

… carry detailed information about sensitivity of individual experimental data points to PDFs; can be studied using statistical packages (TensorFlow, Mathematica,…)

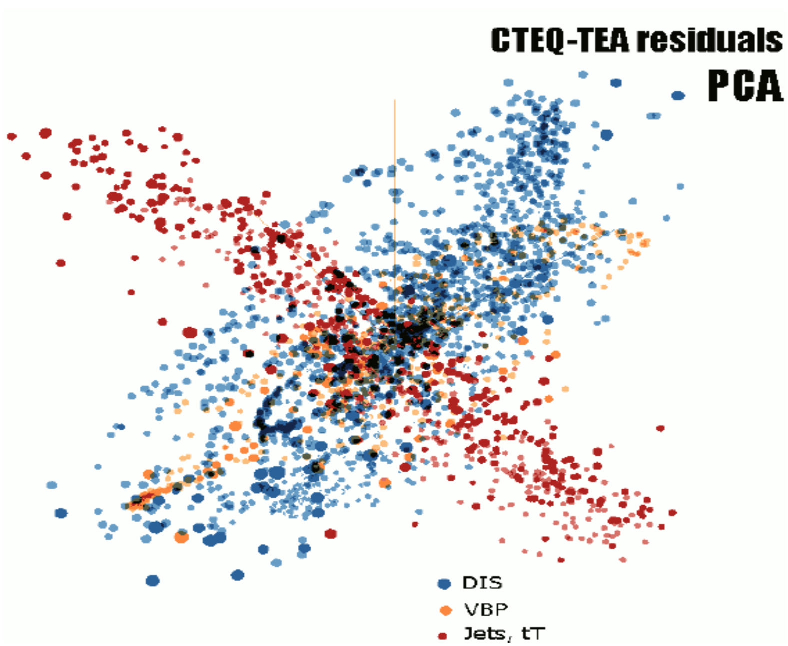

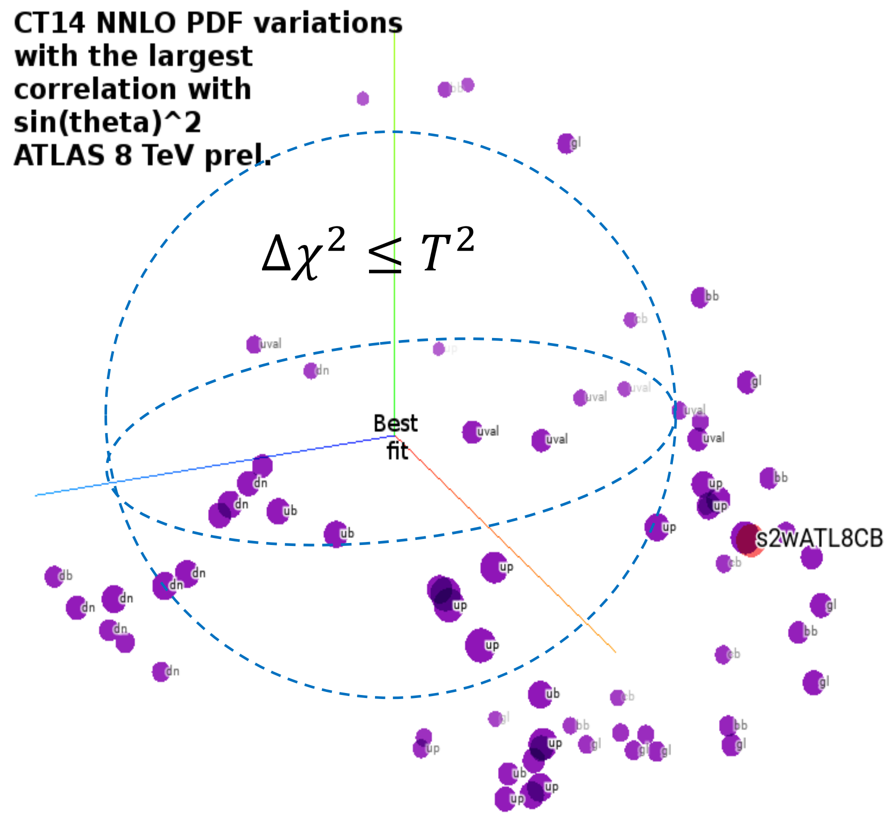

Principal Component Analysis (PCA) visualizes the 56-dim. manifold by reducing it to 10 dimensions (à la META PDFs)

Using Hessian PDFs

A shifted residual r_i

$r_i(\vec{a}) = \frac{T_i(\vec{a}) - D_i^{sh}(\vec{a})}{s_i}$ are N_{pt} **shifted residuals** for point i, PDF parameters $\vec{a}$

$\bar{\lambda}_\alpha(\vec{a})$ are N_λ **optimized nuisance parameters** (dependent on $\vec{a}$)

The $\chi^2(\vec{a})$ for experiment E is

$$\chi^2(\vec{a}) = \sum_{i=1}^{N_{pt}} r_i^2(\vec{a}) + \sum_{\alpha=1}^{N_\lambda} \bar{\lambda}_\alpha^2(\vec{a}) \approx \sum_{i=1}^{N_{pt}} r_i^2(\vec{a})$$

$T_i(\vec{a})$ is the theory prediction for PDF parameters $\vec{a}$

D_i^{sh} is the data value **including the optimal systematic shift**

$$D_i^{sh}(\vec{a}) = D_i - \sum_{\alpha=1}^{N_\lambda} \beta_{i\alpha} \bar{\lambda}_\alpha(\vec{a})$$

s_i is the uncorrelated error

$r_i(\vec{a})$ and $\bar{\lambda}_\alpha(\vec{a})$ are tabulated or extracted from the cov. matrix

Finding shifted residuals r_i from the covariance matrix

The CTEQ-TEA fit returns tables of $r_i(\vec{a})$ and $\bar{\lambda}_\alpha(\vec{a})$ for every i and α

Alternatively, they can be found from the covariance matrix:

$$r_i(\vec{a}) = s_i \sum_{j=1}^{N_{pt}} (\mathrm{cov}^{-1})_{ij} \, (T_j(\vec{a}) - D_j) \,, \qquad \bar{\lambda}_\alpha(\vec{a}) = \sum_{i,j=1}^{N_{pt}} (\mathrm{cov}^{-1})_{ij} \frac{\beta_{i\alpha}}{s_i} \frac{(T_j(\vec{a}) - D_j)}{s_j}$$

Vectors of data residuals

For every data point i, construct a vector of residuals $r_i(\vec{a}_k^{\pm})$ for 2N Hessian eigenvectors. $\mathrm{k} = 1, \ldots, N$, with $N = 28$ for CT14 NNLO:

$$\vec{\delta}_i = \{\delta_{i,1}^{+}, \delta_{i,1}^{-}, \ldots, \delta_{i,N}^{+}, \delta_{i,N}^{-}\} \quad [\mathrm{N} = 28]$$
$$\delta_{i,k}^{\pm} \equiv \left(r_i(\vec{a}_k^{\pm}) - r_i(\vec{a}_0)\right)/\langle r_0 \rangle_E$$

-- a 56-dim vector normalized to $\langle r_0 \rangle_E$, the root-mean-squared residual for the experiment E for the central fit $\vec{a}_0$

$$\langle r_0 \rangle_E \equiv \sqrt{\frac{1}{N_{pt}} \sum_{i=1}^{N_{pt}} r_i^2(\vec{a}_0)} \approx \sqrt{\frac{\chi_E^2\,(\vec{a}_0)}{N_{pt}}}$$

$\langle r_0 \rangle_E \approx 1$ in a good fit to E

r_i is defined in the backup

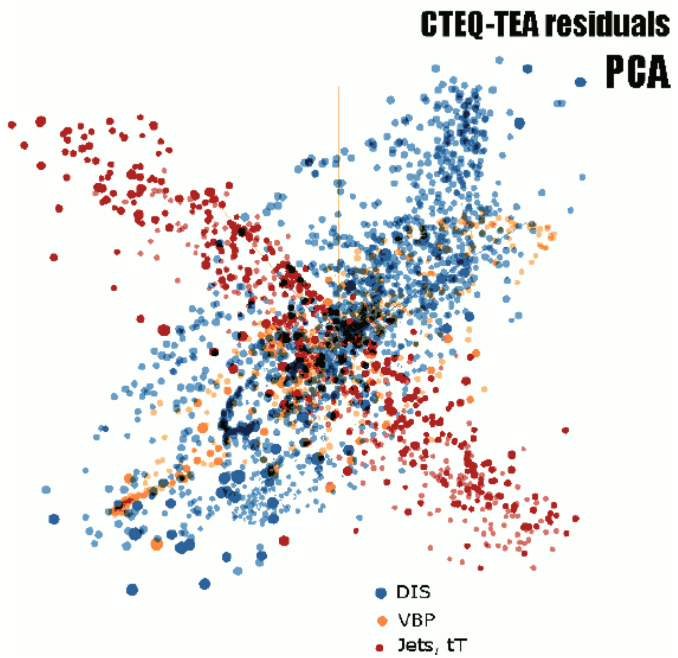

The TensorFlow Embedding Projector (http://projector.tensorflow.org) represents CT14HERA2 $\vec{\delta}_i$ vectors by their 10 principal components indicated by scatter points. A sample 3-dim. projection of the 56-dim. manifold is shown above. A symmetric 28-dim. representation can be alternatively used.

Correlation C_f and sensitivity S_f

The relation of data point i on the PDF dependence of f can be estimated by:

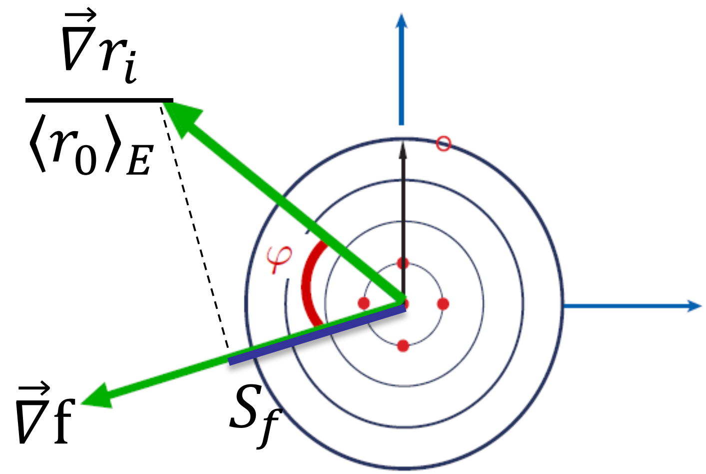

- $C_f \equiv \mathrm{Corr}[\rho_i(\vec{a})), f(\vec{a})] = cos\varphi$

$\vec{\rho}_i \equiv \vec{\nabla} r_i / \langle r_0 \rangle_E$ -- gradient of r_i normalized to the r.m.s. average residual in expt E;

$$\left(\vec{\nabla} r_i\right)_k = \left(r_i(\vec{a}_k^+) - r_i(\vec{a}_k^-)\right)/2$$

C_f is **independent** of the experimental and PDF uncertainties. In the figures, take $|C_f| \gtrsim 0.7$ to indicate a large correlation.

- $S_f \equiv |\vec{\rho}_i| cos\varphi = C_f \frac{\Delta r_i}{\langle r_0 \rangle_E}$ -- projection of $\vec{\rho}_i(\vec{a})$ on $\vec{\nabla} f$

S_f is proportional to $\cos\varphi$ and the ratio of the PDF uncertainty to the experimental uncertainty. We can sum $|S_f|$.
In the figures, take $|S_f| > 0.25$ to be significant.

Sensitivity of hadronic experiments to PDFs

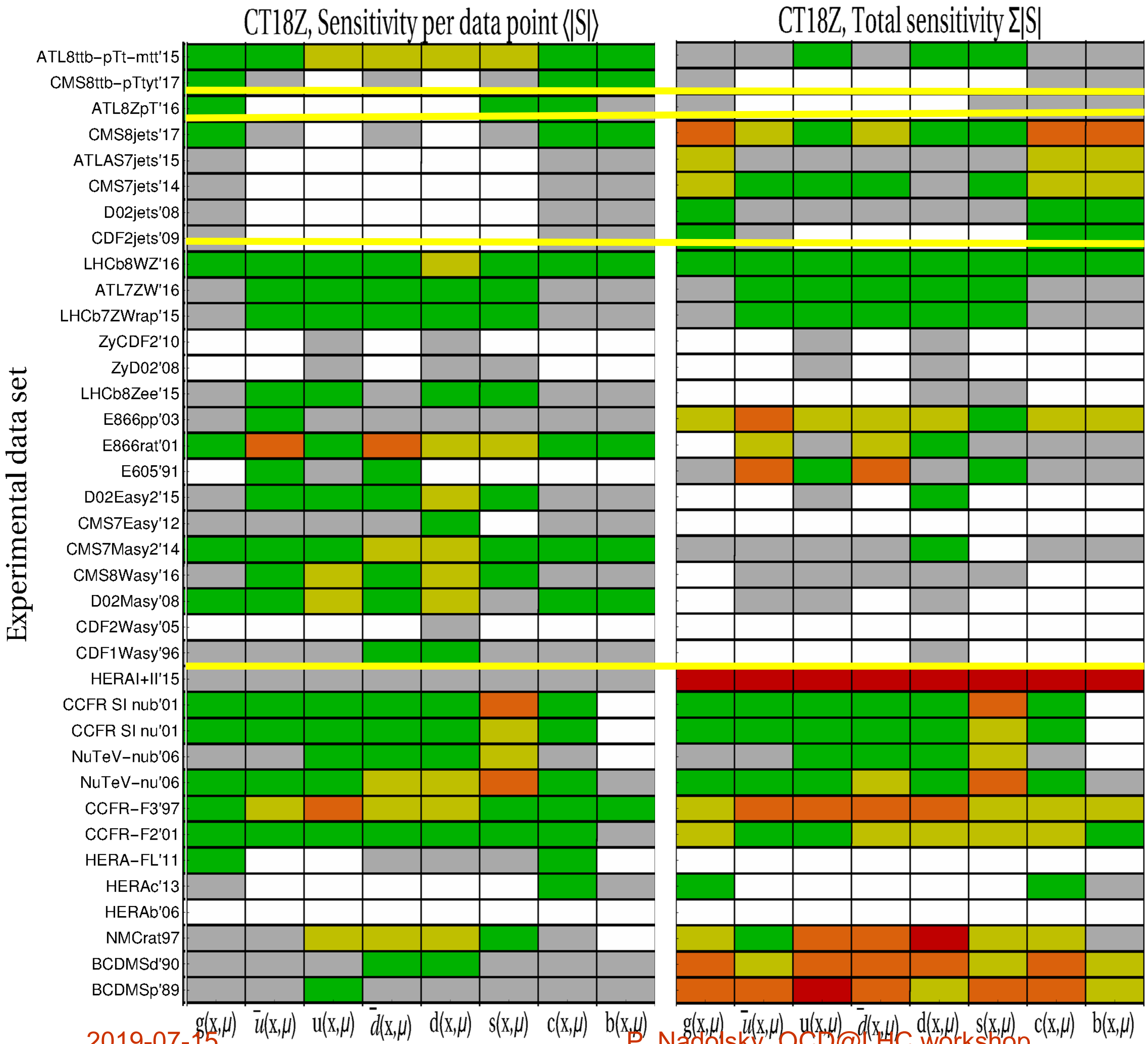

For the CT18Z NNLO data set

Weak (common) goodness-of-fit (GOF) criterion

Based on the global χ^2

A fit of a PDF model to N_{exp} experiments with N_{pt} points ($N_{pt} \gg 1$) is good at the probability level p if $\chi^2_{global} \equiv \sum_{n=1}^{N_{exp}} \chi^2_n$ satisfies

$$P\left(\chi^2 \geq \chi^2_{global}, N_{pt}\right) \geq p; \qquad e.g.$$

$$\left|\chi^2_{global} - N_{pt}\right| \lesssim \sqrt{2N_{pt}} \text{ for } p = 0.68$$

Even when the weak GOF criterion is satisfied, parts of data can be poorly fitted

Then, **tensions between experiments** may lead to **multiple solutions** or **local χ^2 minima** for some PDF combinations

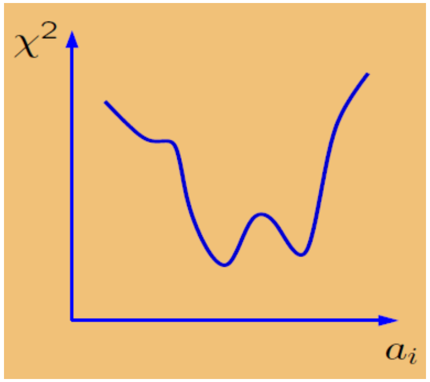

Strong GOF criterion

Shatter the global data set into N_{part} partitions with $N_{pt,n}$ points each

$$1 \le N_{part} \le N_{pt}$$

$$\sum_{n=1}^{N_{part}} N_{pt,n} = N_{pt}$$

A fit is good for this arrangement iff the weak GOF criterion is satisfied for every partition. That is, for each partition n:

- differences between theory and data are indistinguishable from random fluctuations
- $P(\{\chi_n^2\}) \ge 0.68$ for the distribution of χ_n^2 over N_{part} partitions

A fit is close to the ideal when this condition is satisfied for many shattering arrangements

Effective Gaussian variables

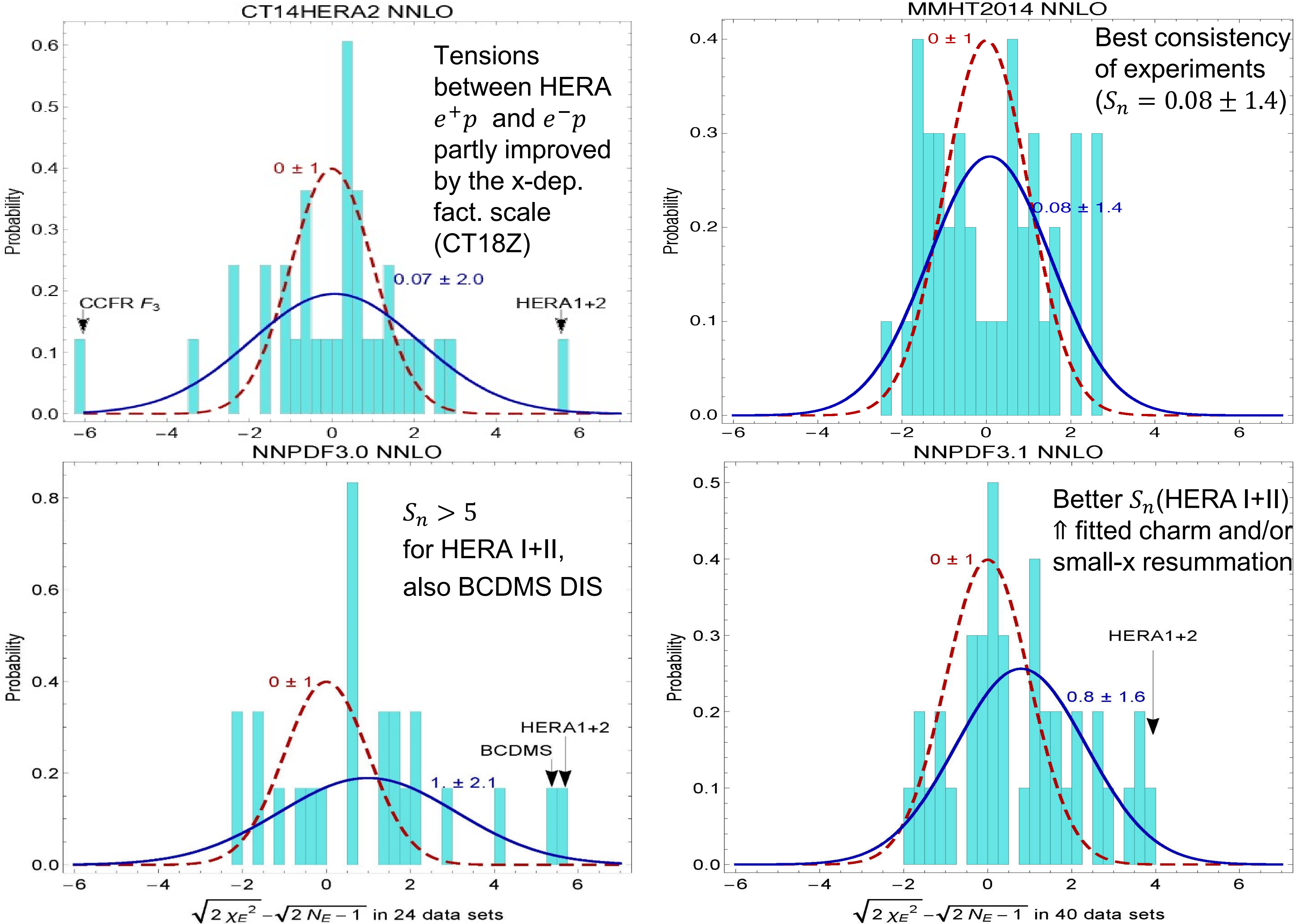

CT14 PDFs with HERA1+2 (=HERA2) combination

Phys.Rev. D95 (2017) 034003

Separate the four HERA2 DIS processes;
(Q_{cut} = 2 GeV)

	N_{pts}	$\chi^2_{red.} / N_{pts}$
NC e^+p	880	1.11
CC e^+p	39	1.10
NC e^-p	159	1.45
CC e^-p	42	1.52
totals		
[reduced χ^2] /N	1120	1.17
χ^2 / N	1120	1.25
R^2 / N	1120	0.08

e^+p data are fitted fine

e^-p data are fitted poorly

reduced χ^2 values

χ^2 = [reduced χ^2] + R^2

The quadratic penalty for 162 systematic errors = 87.5

Fair (not perfect) agreement

CT14 PDFs with HERA1+2 (=HERA2) data

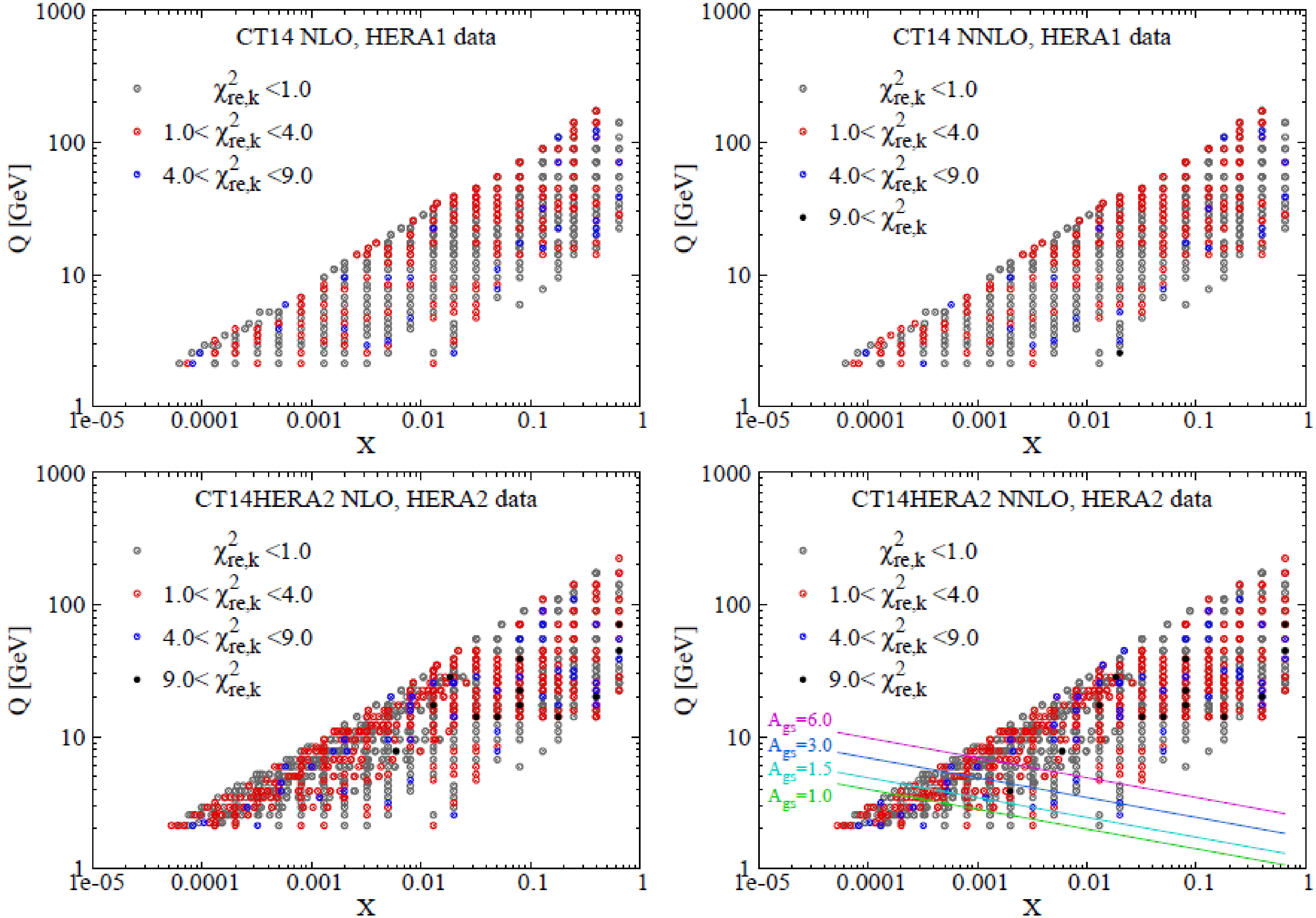

Points with excessive χ^2 are randomly scattered in the $\{x, Q\}$ plane

CTEQ-TEA recommendations for LHC DY measurements Final, page 1 [summary in the CT18 paper]

1. CT18 NNLO or CT14HERA2 NNLO
2. CT18 fits find contradictory preferences for strangeness $x \geq 10^{-3}$ between fitted (SI)DIS experiments, on one hand, and some LHC experiments, especially ATLAS W/Z production measurements and to some extent LHCb W/Z measurements. Benchmarking of LHC measurements and theoretical predictions, as well as new (SI)DIS experiments can be highly effective for resolving these tensions.
3. Theoretical programs for DY processes used in CT18 NNLO are summarized above. The NNLO cross sections for DY are obtained by multiplying fast NLO cross sections by tabulated point-by-point NNLO/NLO ratios (close to 1 in DY processes) computed for a recent CTXX PDF set. Parton shower effects are very limited, especially when NNLO predictions are used.
4. Alternative candidate fits of the CT18 NNLO analysis estimate the QCD scale and numerical uncertainties in high-p_T Z production. In our opinion, NNLO theoretical uncertainties are under good control in the fitted region $50 < p_{TZ} < 150$ GeV of the high-p_T Z production data in the CT18 NNLO analysis.
5. The photon PDFs do not significantly affect the inclusive QCD observables included in the CT18 NNLO analysis.

CTEQ-TEA recommendations for LHC DY measurements Final, page 2

6. When it is relevant, QCD predictions using CT18/CT14 PDFs must use the SACOT-chi scheme and the same charm and bottom mass values as those used to fit the CT18 PDFs. For the LHC observables with all scales much larger than the c, b masses, the S-ACOT-chi hard cross section coincides with the zero-mass MSbar hard cross section. On the other hand, the mass effects may be relevant in W/Z p_T distributions in c, b channels at $p_T^2 \lesssim m_{c,b}^2$. A comprehensive study of the power-suppressed/intrinsic/fitted charm distribution is published in **JHEP 1802 (2018) 059 / arXiv:1707.00657.** CTEQ-TEA does not see it mandatory to use the fitted charm parametrizations throughout. The PDFs with fitted charm such as CT14 IC or NNPDF3.1 do not provide a better theoretical framework than the standard CT14 PDFs. A large part of the fitted charm PDF may arise from twist-4 contributions that are unique to low-Q DIS.
7. The TMD effects are negligible in the recent CTEQ-TEA analyses.
8. No, various kinds of parametrization and methodological uncertainties are accounted for in the CTEQ-TEA PDF errors and are studied regularly as a part of the CTEQ-TEA analysis.

CTEQ-TEA recommendations for LHC DY measurements Final, page 3

9. As of 2018, we do not recommend to fit the PDFs only to the LHC or DY data. The most significant constraints arise from other experiments, such as fixed-target DIS. It is ok to perform this type of study with a reduced number of data sets as a benchmarking exercise among the PDF groups, but the resulting PDFs will be less accurate/precise than the global PDF fits.
10. To a great degree, the important uncertainties, those due to the experimental errors of the datasets included in the fit, are already completely correlated. Correlation of other issues, such as parameterizations/scale choices can be studied.
11. If the PDF sets include the data, but do not agree with the data, and the other PDF sets do, then it is crucial to understand the source of the disagreement.
12. If the measurements do not have clearly defined systematic errors (in the modern sense), then it is justified to not use them in a global PDF fit. If the data sets are in strong tension with the other data sets used in a global fit, then they can be excluded. Of course, this happens on a case-by-case basis.

CTEQ-TEA recommendations for LHC DY measurements Final, page 4

13. The Hessian and MC approaches are complementary. In recent years, the PDF groups have gained a great deal of experience in converting between Hessian and MC replica PDFs, strengthening the understanding of both. The Hessian PDFs are sufficient for the majority of estimates of PDF uncertainty in the case of sufficient experimental constraints. The MC error PDFs are useful in the case of weak experimental constraints or persistent non-Gaussian effects.
14. Conceptual foundations of PDF reweighting have not been explored sufficiently, which may result in its spurious applications. This area needs additional exploration before PDF reweighting can be safely used in high-stake situations such as in item 11.